TS-insoluble pellets were lysed in TS buffer containing 1% (v/v) TX, and centrifuged at 290,000×g for 20 min at 4 °C. The supernatant was collected as TX-soluble fraction. TX-insoluble pellets were further sonicated in TS buffer containing 1% (w/v) Sarkosyl (Sar), and incubated for 30 min at 37 °C. The mixtures were centrifuged at 290,000×g for 20 min at room temperature, and the supernatant was recovered as the Sar-soluble fraction. The remaining pellets (insoluble in Sar) were lysed in SDS-sample buffer and heated for 5 min.

Each sample (10 or 20 μg) was separated by 12% (v/v) SDS–PAGE using Tris–glycine buffer system, and proteins were transferred onto polyvinylidene difluoride membrane (Millipore). The blots were incubated overnight with the indicated primary antibody at an appropriate dilution (1:1000–3000) at room temperature, followed by the incubation with a biotin-labeled secondary antibody. Signals were detected using an ABC staining kit (Vector).

2.6. CFTR exon 9 skipping assay

Cos-7 cells in 6-well plates were transfected with 0.5 μg of the reporter plasmid pSPL3-CFTR9 plus 1 μg of pcDNA3 plasmid encoding wild-type or its mutants, using FuGENE6. The cells were harvested 48 h post transfection, and total RNA was extracted with TRIzol (Invitrogen). The cDNA was synthesized from 1 μg of total RNA with the use of the Superscript II system (Invitrogen). Primary and secondary PCRs were carried out according to the instruction manual of the exon trapping system (Life Technologies).

3. Results

3.1. Effect of deletion of two candidate NLS in TDP-43

Amino acid sequence containing proline followed by a cluster of basic amino acids is known to be typical NLS. We found two such sequences in TDP-43, PKDNKRK (residues 78–84) and PLRSRK (residues 187–192) (Fig. 1A). To examine whether these sequences function as the NLS, we constructed corresponding deletion mutants of TDP-43 and expressed them in SH-SY5Y cells. We employed non-tagged TDP-43 plasmid for expression in cultured cells, since expression of hemagglutinin (HA)-tagged TDP-43 in SH-SY5Y cells caused formation of inclusion-like structures (Fig. S1), suggesting that addition of the epitope tag to the N-terminus may affect the conformation of TDP-43 and promote non-specific aggregate formation.

Endogenous TDP-43 expressed in the nucleus (Fig. 1B). Similar but stronger nuclear TDP-43 staining was observed in cells expressing wild-type TDP-43 (Fig. 1C), as compared with non-transfected cells (Fig. 1B). When the deletion mutant lacking residues 78–84 (ΔNLS) was transiently expressed, strong TDP-43 signals were detected in cytoplasm (Fig. 1D). This is reasonable because the sequence of 78–84 contains a part of the bipartite NLS in TDP-43 recently identified by Winton et al. [7].

When the deletion mutant lacking residues 187–192 (Δ187–192) was expressed, on the other hand, the mutant protein formed dot-like structures in nuclei (Fig. 1E). This observation suggests that this sequence does not function as a NLS.

3.2. Formation of intracellular TDP-43 inclusions in cultured SH-SY5Y cells

Impaired Ub–proteasome system has been suggested in some forms of neurodegenerative disease [8], and TDP-43 is indeed ubiquitinated in the brains of patients with FTLD-U or ALS [3]. To examine whether impaired Ub–proteasome system is involved in inclusion formation, we treated cells transfected with TDP-43 wild-type or deletion mutants with a proteasome inhibitor, MG132. In immunocytochemistry using phosphorylation-independent anti-TDP-43 antibody, no obvious change in the localization of TDP-43 was observed in mock cells (Fig. 2A), or in cells transfected with wild-type (Fig. 2B) or ΔNLS mutant (Fig. 2C) after MG132 treatment, as compared to those without MG132 (Fig. 1). In contrast, many round nuclear inclusions were generated in cells transfected with Δ187–192 mutant after MG132 treatment (Fig. 2D: ~12% of inclusion-positive cells).

Fig. 3 revealed the results of double immunostaining using anti-pS409/410, phosphorylation-dependent anti-TDP-43 antibody [6], and anti-Ub antibody. Cells expressing wild-type TDP-43 showed

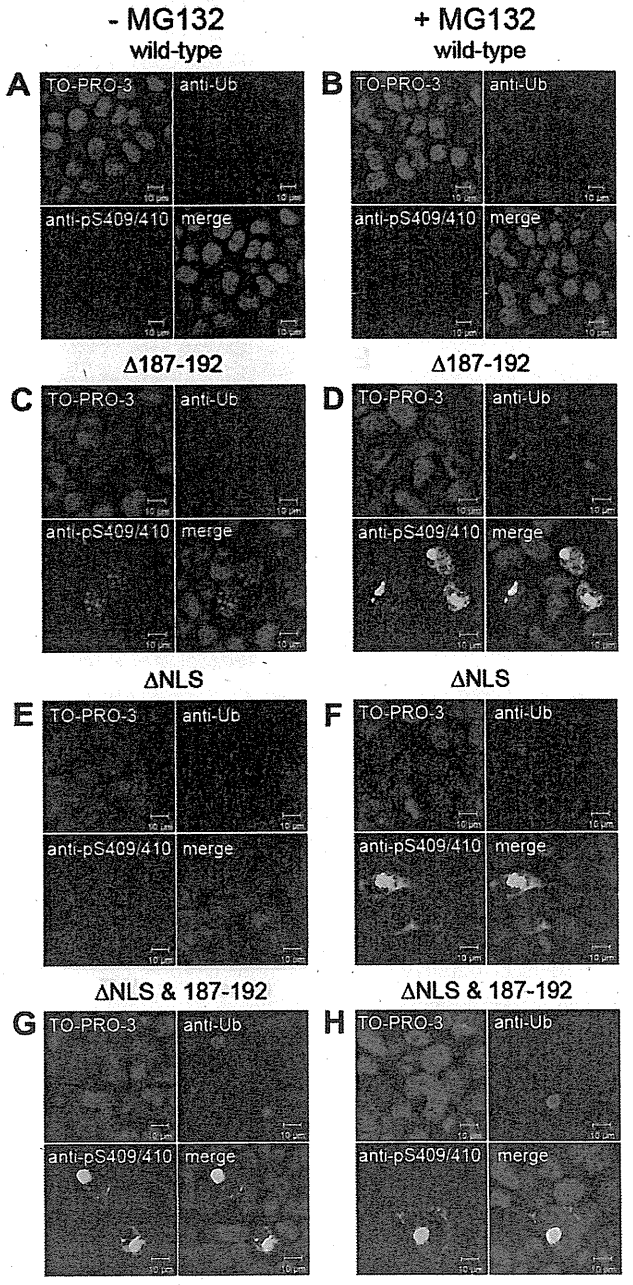

Fig. 3. Immunocytochemical analyses of intracellular inclusion-like structures formed in cells transfected with deletion mutants of TDP-43. SH-SY5Y cells 72 h post transfection with wild-type, (A and B), Δ187–192 (C and D), ΔNLS (E and F), and ΔNLS&187–192 (G and H) before (A, C, E, G) and after (B, D, F, H) treatment with MG132 (20 μM for 6 h) were stained with a phosphorylation-specific antibody, anti-pS409/410 (green), anti-ubiquitin (Ub: red) antibodies, and TO-PRO-3 (blue).

no immunoreactivity for anti-pS409/410 and anti-Ub antibodies in the presence or absence of MG132 (Fig. 3A and B). Cells transfected with Δ187–192 showed small dot-like structures positive for anti-pS409/410 antibody but negative for anti-Ub antibody without MG132 treatment (Fig. 3C). Cells transfected with Δ187–192 after the MG132 treatment contained inclusion-like structures in nuclei that were intensely labeled with both antibodies (Fig. 3D: ~8% of inclusion-positive cells). Relatively large inclusions (~5 μm) were immunopositive for both antibodies, while small ones (<1 μm) were positive for only phospho-specific TDP-43 antibody, suggesting that abnormal phosphorylation of TDP-43 is an early event in the process of inclusion formation.

Cells transfected with ΔNLS showed no immunoreactivity without MG132 treatment (Fig. 3E), but showed formation of cytoplasmic inclusions positive for both anti-pS409/410 and anti-Ub after MG132 treatment (Fig. 3F: ~10% of inclusion-positive cells). Furthermore, cells transfected with mutant TDP-43 lacking both the NLS and residues 187–192, named ΔNLS&187–192, formed intracellular round inclusion-like structures positive for both anti-pS409/410 and anti-Ub antibodies, independently of treatment

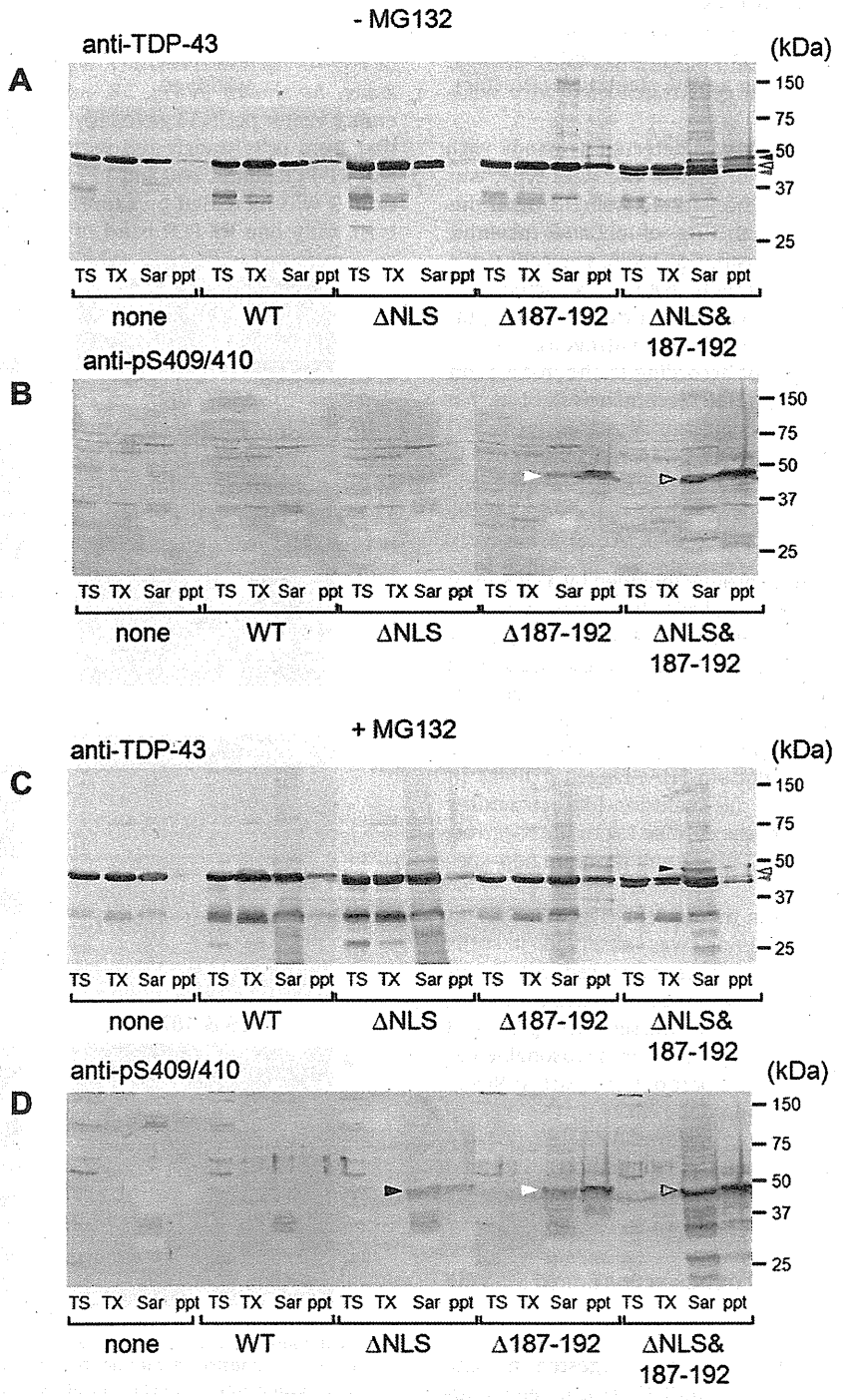

Fig. 4. Immunoblot analyses of intracellular inclusions of deleted TDP-43 mutants in SH-SY5Y cells. Untransfected cells (none) and cells 72 h post transfection with wild-type (WT) or TDP-43 deletion mutants, before (A and B) and after (C and D) treatment with MG132 (1 μM overnight), were sequentially extracted with Tris–saline (TS), 1% Triton-X (TX) and 1% Sarkosyl (Sar), and these supernatants and the Sarkosyl-insoluble pellets (ppt) were run on SDS–PAGE, transferred to PVDF membrane and probed with anti-TDP-43 antibody (A and C) and anti-pS409/410 (B and D).

with MG132 (Fig. 3G: ~8% of inclusion-positive cells and H: ~12% of inclusion-positive cells). The inclusions were ~10 μm in diameter, being very similar in size to the neuronal cytoplasmic inclusions found in patients with FTLD-U [2].

3.3. Immunoblot analysis of intracellular inclusions in the cultured cell models

Cells expressing wild-type or mutant TDP-43 were sequentially extracted, and the supernatants and pellets were analyzed by immunoblotting. On analysis of cell lysates using anti-TDP-43 antibody, endogenous TDP-43 at 43 kDa was detected in all fractions. Immunoreactivity of it was the strongest in TX-soluble fraction, and was the weakest in Sar-insoluble fraction (black-lined arrowheads in Fig. 4A and C). A similar band pattern but with stronger immunoreactivities was detected in cells transfected with wild-type TDP-43 (WT).

The ΔNLS mutant TDP-43, which was detected as bands with slightly lower molecular weight than that of the wild-type, was also recovered mostly in the TS- and TX-soluble fractions (Fig. 4A). The intensities of bands in the Sar-soluble and -insoluble fractions were slightly increased after MG132 treatment (Fig. 4C). Interestingly, these were positive for anti-pS409/410 (a black arrowhead in Fig. 4D), suggesting that inhibition of proteasome activity induces the aggregation of phosphorylated ΔNLS.

In contrast, expression of Δ187–192 mutant TDP-43, which was detected as a band with almost the same molecular weight as that of endogenous TDP-43, resulted in significant increases in the Sar-soluble and -insoluble (ppt) fractions as compared with those in cells transfected with wild-type TDP-43 (Fig. 4A). Smeared and higher-molecular-weight bands were also detected in the Sar-soluble and -insoluble fractions (Fig. 4A). We also observed pS409/410-positive bands in the Sar-soluble and -insoluble fractions in the absence or presence of MG132 (white arrowheads in Fig. 4B and D).

Finally, immunoblots of lysates from cells expressing ΔNLS&187–192 mutant TDP-43 (~41 kDa bands marked with grey arrowheads in Fig. 4A and C) showed high-molecular-weight bands of ~45 kDa (black arrowheads in Fig. 4A and C) and smears in the Sar-soluble and -insoluble fractions. The bands of ~45 kDa, smears, and C-terminal fragments at 25–37 kDa were highly immunoreactive with anti-pS409/410 antibody independently of MG132 treatment (black-lined arrowheads in Fig. 4B and D). These were similar characteristic band patterns to those found in immunoblot analyses of brain lysates of FTLD-U and ALS as previously reported [6].

3.4. Deletion mutants of TDP-43 lost the exon skipping activity

To evaluate the functional significance of the deletion mutants of TDP-43 used in this study, we performed CFTR exon 9 skipping assay. As shown in Fig. 5B, mRNA from cells transfected with empty vector pcDNA3 gave only one RT-PCR band of 360 bp, while that from cells transfected with pcDNA3-TDP-43 wild-type gave two RT-PCR bands, 360 and 177 bp, showing that skipping of CFTR exon 9 was increased by expression of wild-type TDP-43. In contrast, only one RT-PCR band of 360 bp was observed from cells co-transfected with ΔNLS, Δ187–192, or ΔNLS&187–192, indicating that these mutants do not have skipping activity of CFTR exon 9, which is one of known physiological functions of TDP-43.

4. Discussion

In this study, using SH-SY5Y cells and a phosphorylated TDP-43 specific antibody established by ourselves, we examined the effect of deletion of two candidate sequences for NLS, residues 78–84 and 187–192 of TDP-43, and proteasomal inhibition on inclusion formation. Mislocalization of TDP-43 into cytoplasm caused by deletion of residues 78–84 proves that this sequence indeed functions as NLS. This result is largely consistent with the previous report by Winton et al., which showed that residues 82–98 were

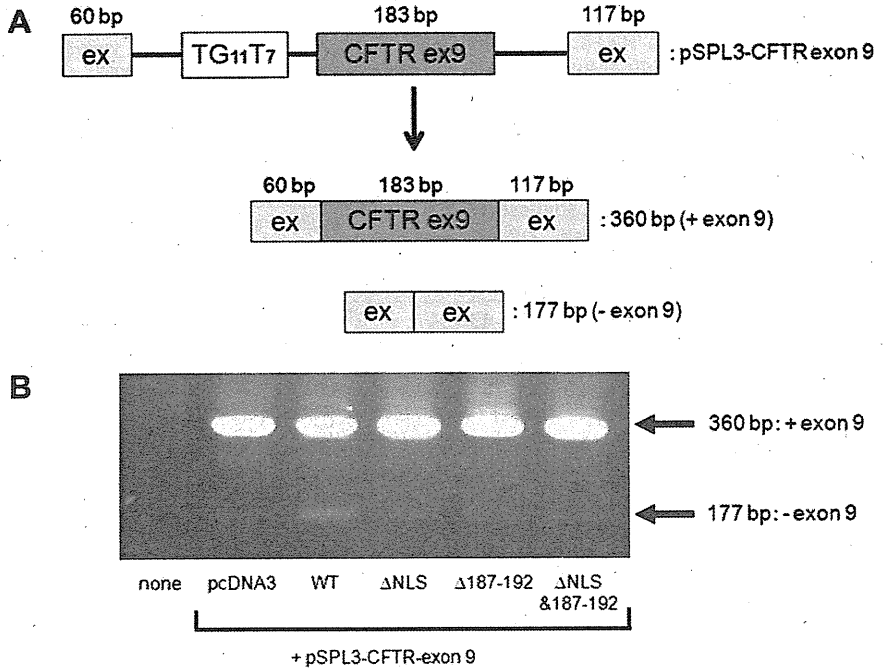

Fig. 5. CFTR exon 9 skipping assay of the deletion mutants of TDP-43. (A) Schematic diagram of the reporter plasmid pSPL3-CFTR exon 9. This plasmid contains the repeat sequence of TG11T7 in which the TG11 repeat is recognized by TDP-43, causing the CFTR exon 9 to be spliced out. The insert of this plasmid contains two exons of HIV-1 tat gene (60 and 117 bp, respectively: light grey boxes) flanking CFTR exon 9 (183 bp: a dark grey box). RT-PCR is expected to generate two products with (360 bp) and without CFTR exon 9 (177 bp). (B) Gel electrophoresis of RT-PCR products of RNA from transfected cos-7 cells. The RNAs from cos-7 cells, co-transfected with the reporter plasmid pSPL3-CFTR exon 9 plus pcDNA3 expression vectors were used as templates for RT-PCR analysis. The products were analyzed by electrophoresis in 1.5% agarose gel.

required for TDP-43 entry into the nucleus [7]. Formation of intranuclear TDP-43 positive dot-like structures caused by deletion of residues 187–192 suggests that this sequence does not function as a NLS but is nonetheless important to maintain a physiological state of TDP-43 in the nucleus. Loss of the exon skipping activity of CFTR exon 9 observed in cells transfected with this mutant may also support such a notion.

The results of the present study suggest that mislocalization of TDP-43 in cytoplasm is not a sufficient condition for aggregation of TDP-43, since the treatment of MG132, a proteasomal inhibitor, is needed to cause the formation of inclusion in cells transfected with a mutant TDP-43 lacking residues 78–84. Proteasome inhibition also induced formation of intranuclear inclusions in cells transfected with a mutant TDP-43 lacking residues 187–192. These results also suggest that a proteasome activity plays an important role for degradation of TDP-43. Impairment of the ubiquitin-proteasome system has recently been suggested to be related to the onset of neurodegenerative diseases. For instance, Bence et al reported that intracellular aggregates of a huntingtin fragment containing a pathogenic polyglutamine repeat directly impaired the function of the ubiquitin-proteasome system [9]. Keck et al., showed that proteasome was inhibited by paired helical filament-tau in brains of patients with Alzheimer's disease [10]. It should be further investigated whether the proteasome activity is actually decreased in brains of patients with TDP-43 proteinopathies, as Keller et al., reported that a significant decrease in proteasome activity was observed in AD brains [11]. Function of autophagy-lysosome degradation system may be an issue to be investigated as well, since inhibition of autophagic degradation by depletion of the endosomal sorting complexes required for transport (ESCRT) subunits causes accumulation of TDP-43 in ubiquitinated inclusions in cultured cells [12].

In contrast to a mutant lacking residues 78–84 or 187–192, double-deletion mutant of these sequences caused inclusion formation without proteasomal inhibition in this study. These results suggest the possibility that the double mutant protein has a higher propensity to aggregate than each single mutant protein. In this context, it should be noted that in insoluble fraction from FTLD-U brains, the amount of C-terminal fragments of TDP-43 is higher than that of the full-length TDP-43 [6]. These findings suggest that conformation or modifications of TDP-43 is another important factor for inclusion formation.

Importantly, intranuclear or cytoplasmic inclusions observed in this study were immunopositive for both a phosphorylation-dependent anti-TDP-43 antibody and anti-Ub antibody, suggesting that those consist of phosphorylated and ubiquitinated TDP-43. Biochemical analyses also support that abnormal phosphorylation of TDP-43 takes place in cells with inclusions. These results suggest that our cellular models recapitulate the phenotypes of TDP-43 proteinopathies both pathologically and biochemically. These models are expected to be valuable tools for understanding the pathological process underlying TDP-43 proteinopathies and for identifying candidate drugs to prevent intracellular aggregation of TDP-43.

Acknowledgements

We thank Dr. M. Arai (Tokyo Institute of Psychiatry) for providing human genomic DNA, and Drs. H. Mimuro (University of Tokyo) and F. Kametani (Tokyo Institute of Psychiatry) for helpful advice and discussions. This work was supported by a Grant-in-Aid for Scientific Research on Priority Areas-Research on Pathomechanisms of Brain Disorders (to M.H., 20023038) and Grants-in-Aid for Scientific Research (B) (to M.H., 18300117) and (C) (to T.N., 19590297 and T.A., 19591024) from the Ministry of Education, Culture, Sports, Science and Technology of Japan.

Appendix A. Supplementary data

Supplementary data associated with this article can be found, in the online version, at doi:10.1016/j.febslet.2008.12.031.

References

[1] Snowden, J.S., Neary, D. and Mann, D.M. (2002) Frontotemporal dementia. Brit. J. Psychiatr. 180, 140–143.
[2] Arai, T. et al. (2006) TDP-43 is a component of ubiquitin-positive tau-negative inclusions in frontotemporal lobar degeneration and amyotrophic lateral sclerosis. Biochem. Biophys. Res. Commun. 351, 602–611.
[3] Neumann, M. et al. (2006) Ubiquitinated TDP-43 in frontotemporal lobar degeneration and amyotrophic lateral sclerosis. Science 314, 130–133.
[4] Ou, S.H., Wu, F., Harrich, D., Garcia-Martinez, L.F. and Gaynor, R.B. (1995) Cloning and characterization of a novel cellular protein, TDP-43, that binds to human immunodeficiency virus type 1 TAR DNA sequence motifs. J. Virol. 69, 3584–3596.
[5] Buratti, E., Dork, T., Zuccato, E., Pagani, F., Romano, M. and Baralle, F.E. (2001) Nuclear factor TDP-43 and SR proteins promote in vitro and in vivo CFTR exon 9 skipping. EMBO J. 20, 1774–1784.
[6] Hasegawa, M. et al. (2008) Phosphorylated TDP-43 in frontotemporal lobar degeneration and amyotrophic lateral sclerosis. Ann. Neurol. 64, 60–70.
[7] Winton, M.J., Igaz, L.M., Wong, M.M., Kwong, L.K., Trojanowski, J.Q. and Lee, V.M. (2008) Disturbance of nuclear and cytoplasmic TAR DNA-binding protein (TDP-43) induces disease-like redistribution, sequestration, and aggregate formation. J. Biol. Chem. 283, 13302–13309.
[8] Giasson, B.I. and Lee, V.M. (2003) Are ubiquitination pathways central to Parkinson's disease? Cell 114, 1–8.
[9] Bence, N.F., Sampat, R.M. and Kopito, R.R. (2001) Impairment of the ubiquitin–proteasome system by protein aggregation. Science 292, 1552–1555.
[10] Keck, S., Nitsch, R., Grune, T. and Ullrich, O. (2003) Proteasome inhibition by paired helical filament-tau in brains of patients with Alzheimer's disease. J. Neurochem. 85, 115–122.
[11] Keller, J.N., Hanni, K.B. and Markesbery, W.R. (2000) Impaired proteasome function in Alzheimer's disease. J. Neurochem. 75, 436–439.
[12] Filimonenko, M. et al. (2007) Functional multivesicular bodies are required for autophagic clearance of protein aggregates associated with neurodegenerative disease. J. Cell Biol. 179, 485–500.

Acta Neuropathol (2010) 120:55–66
DOI 10.1007/s00401-010-0702-1

ORIGINAL PAPER

Phosphorylated TDP-43 pathology and hippocampal sclerosis in progressive supranuclear palsy

Osamu Yokota · Yvonne Davidson · Eileen H. Bigio · Hideki Ishizu · Seishi Terada · Tetsuaki Arai · Masato Hasegawa · Haruhiko Akiyama · Stephen Sikkink · Stuart Pickering-Brown · David M. A. Mann

Received: 15 March 2010 / Revised: 20 May 2010 / Accepted: 21 May 2010 / Published online: 30 May 2010

Abstract TDP-43 is characteristically accumulated in TDP-43 proteinopathies such as frontotemporal lobar degeneration and motor neurone disease, but is also present in some tauopathies, including Alzheimer's disease, argyrophilic grain disease, and corticobasal degeneration (CBD). However, several studies have suggested that cases of progressive supranuclear palsy (PSP) lack TDP-43 pathology. We have therefore examined limbic regions of the brain in 19 PSP cases, as well as in 12 CBD cases, using phosphorylation-dependent anti-TDP-43 antibodies. We observed TDP-43-positive inclusions in five PSP cases (26%), as well as in two CBD cases (17%). The amygdala and hippocampal dentate gyrus were most frequently affected in PSP. Regional tau burden tended to be higher in TDP-43-positive PSP cases, and a significant correlation between tau and TDP-43 burden was noted in the occipitotemporal gyrus. Hippocampal sclerosis (HS) was found in 3/5 TDP-43-positive PSP cases, but HS was significantly more frequent in TDP-43-positive than TDP-43 negative PSP cases. Dementia was present in 13/19 (58%) of the PSP cases, in 4/5 TDP-43-positive cases, in all 3 TDP-43-positive cases with HS, in 1/2 TDP-43-positive cases without HS, and 7/14 cases lacking both. TDP-43 and tau were frequently colocalized in the amygdala, but not in the hippocampal dentate gyrus. Immunoblotting demonstrated the characteristic (for TDP-43 proteinopathies) 45 and 25 kDa bands and high molecular weight smear in the TDP-43-positive PSP case. These findings suggest that (1) although PSP is nominally a tauopathy, pathological TDP-43 can accumulate in the limbic system in some cases, and (2) TDP-43 pathology may be concurrent with HS.

O. Yokota · Y. Davidson · D. M. A. Mann (✉)
Neurodegeneration and Mental Health Research Group, Faculty of Medical and Human Sciences, School of Community Based Medicine, Greater Manchester Neurosciences Centre, Hope Hospital, University of Manchester, Salford M6 8HD, UK
e-mail: david.mann@manchester.ac.uk

S. Sikkink · S. Pickering-Brown
Neurodegeneration and Mental Health Research Group, Faculty of Medical and Human Sciences, School of Community Based Medicine, A V Hill Building, University of Manchester, Oxford Rd, Manchester M13 9PL, UK

E. H. Bigio
Department of Pathology, Northwestern University Feinberg School of Medicine, Chicago, IL 60619, USA

O. Yokota · H. Ishizu · S. Terada
Department of Neuropsychiatry, Okayama University Graduate School of Medicine, Dentistry and Pharmaceutical Sciences, 2-5-1 Shikata-cho, Okayama 700-8558, Japan

H. Ishizu
Zikei Institute of Psychiatry, 100-2, Urayasu-honcho, Okayama 702-8508, Japan

T. Arai · H. Akiyama
Department of Psychogeriatrics, Tokyo Institute of Psychiatry, 2-1-8 Kamikitazawa, Setagaya-ku, Tokyo 156-8585, Japan

M. Hasegawa
Department of Molecular Neurobiology, Tokyo Institute of Psychiatry, 2-1-8 Kamikitazawa, Setagaya-ku, Tokyo 156-8585, Japan

Keywords Argyrophilic grains · Hippocampal sclerosis · Progressive supranuclear palsy · Tau · TDP-43

Introduction

Transactivation-responsive DNA-binding protein of M_r 43 kDa (TDP-43) is a nuclear protein involved in transcriptional repression and alternative splicing. It was originally identified as a major component of ubiquitin-positive and tau-negative inclusions in the frontotemporal cortex and motor neurons in frontotemporal lobar degeneration (FTLD-U), with or without progranulin gene mutations, and in amyotrophic lateral sclerosis (ALS) [3, 12, 31]. Subsequent studies revealed that TDP-43 is also abnormally accumulated in familial FTLD-U with mutations in the valosin-containing protein gene [32], in familial FTLD with motor neuron disease linked to chromosome 9p [10], and in ALS with TDP-43 gene mutations [25, 38, 41, 44]. TDP-43 is considered to play an essential pathogenic role in these diseases, now-called TDP-43 proteinopathies.

Although TDP-43 accumulation was originally considered to be a specific disease marker for FTLD-U and ALS, subsequent studies demonstrated that abnormal TDP-43 accumulation in some cases of other neurodegenerative diseases, such as Alzheimer's disease (AD) [2], Parkinson's disease with and without dementia [30], dementia with Lewy bodies (DLB) + AD [4, 30], ALS/parkinson-dementia complex of Guam (ALS/PDC of Guam) [15, 16], argyrophilic grain disease (AGD) [14], and Huntington disease [37]. However, the pathophysiological significance of concurrent TDP-43 accumulation, and its impact on clinical phenotype in these diseases remain unclear.

Several previous studies have suggested that cases of progressive supranuclear palsy (PSP) lack abnormal TDP-43 accumulation [3, 18, 40]. In these early studies, phosphorylation-independent antibodies were employed in TDP-43 immunohistochemistry and immunoblot analysis. We have made polyclonal and monoclonal antibodies specific for phophorylated TDP-43, which identify phosphorylation sites in the C-terminus of the TDP-43 accumulated in FTLD-TDP brains [17, 20], and selectively immunolabel pathological inclusions and dystrophic neurites without physiological nuclear staining in FTLD-TDP, ALS, AD with TDP-43 pathology, and in DLB with TDP-43 [4, 17]. They also recognize hyperphosphorylated TDP-43 at 45 kDa and additional 18–26 kDa fragments in sarkosyl-insoluble fractions on immunoblotting.

The principal aim of this study was to revisit the presence or absence, and the frequency, of TDP-43 pathology in PSP cases using a phosphorylation-dependent anti-TDP-43 antibody. In contrast to previous reports, we demonstrated that a significant proportion of PSP cases had variable degrees of TDP-43 pathology in the limbic system. We subsequently examined the relationships between TDP-43 pathology, tau pathology, and hippocampal sclerosis, as well as biochemical nature of the abnormally accumulated TDP-43, in PSP.

Materials and methods

Subjects

We investigated 19 pathologically confirmed PSP cases, 12 pathologically confirmed corticobasal degeneration (CBD) cases and 4 pathologically normal control subjects (Table 1). These cases were obtained from UK Parkinson's Disease Society Tissue Bank (7 PSP and 4 control cases), Department of Pathology, Northwestern University Feinberg School of Medicine Cognitive Neurology and Alzheimer Disease Center (5 PSP and 7 CBD cases), and Department of Neuropsychiatry, Okayama University Graduate School of Medicine, Dentistry and Pharmaceutical Sciences (7 PSP and 5 CBD cases). All brains had been collected with Local Research Ethical Committee approval. All PSP cases showed characteristic tufted astrocytes, and all CBD cases astrocytic plaques, as revealed by Gallyas-Braak silver methods and tau immunohistochemistry.

Immunohistochemistry

Sections cut at 5-μm thickness to include the amygdala, entorhinal cortex, hippocampus, occipitotemporal cortex in all cases, as well as the substantia nigra in two cases for which tissue was available, were stained with antibodies against phosphorylated TDP-43 (pAb pS409/410, rabbit, polyclonal, 1:1,000 [17]), phosphorylated tau (AT8, mouse, monoclonal, 1:3,000, Innogenetics, Ghent, Belgium), phosphorylated α-synuclein (#1175, rabbit, polyclonal, 1:1,000, [33]), and Aβ (4G8, mouse, monoclonal, 1:2,000, Covance Research Products Inc., Dedham, MA, USA). Deparaffinized sections were incubated with 1% H_2O_2 in methanol for 20 min to eliminate endogenous peroxidase activity in the tissue. When using anti-α-synuclein and anti-TDP-43 antibodies, sections were pretreated to enhance immunoreactivity in a microwave oven for 5 min in 10 mM sodium citrate buffer, pH 6.0, at 100°C. After blocking with 10% normal serum, sections were incubated 1 h at room temperature with the primary antibody. After three 5-min washes in phosphate-buffered saline (PBS), sections were incubated in biotinylated secondary antibody for 30 min, and then in avidin-biotinylated horseradish peroxidase complex (ABC Elite kit, Vector, Burlingame, CA, USA) for

Table 1 Demographic data in PSP and CBD cases with and without TDP-43 pathologies

	PSP			CBD		
	All	TDP-43-positive PSP	TDP-43-negative PSP	All	TDP-43-positive CBD	TDP-43-negative CBD
N (%)	19	5 (26.3)	14 (73.7)	12	2 (16.7)	10 (83.3)
Male [*N* (%)]	16 (84.2)	4 (80.0)	12 (85.7)	7 (58.3)	1 (50.0)	6 (60.0)
Age at onset [mean (SD)]	68.3 (9.8)	75.0 (9.4)	65.7 (9.0)	55.2 (10.2)	49.0 (12.7)	56.6 (9.9)
Age at death [mean (SD)]	76.3 (10.7)	82.4 (11.7)	74.1 (9.8)	62.8 (11.2)	56.0 (15.6)	64.1 (10.7)
Duration [mean (SD)]	7.4 (4.4)	7.4 (4.6)	7.5 (4.6)	7.3 (2.9)	7.0 (2.8)	7.3 (3.1)
Dementia (%)	11 (57.9)	4 (80.0)	7 (50.0)	11 (91.7)	2 (100.0)	9 (90.0)
Brain weight [g, mean (SD)]	1,202 (142)	1,234 (180)	1,190 (132)	1,174 (146)	1,008 (152)	1,215 (120)
Argyrophilic grains [*N* (%)]	4 (21.1)	1 (20.0)	3 (21.4)	3 (25.0)	1 (50.0)	2 (20.0)
Hippocampal sclerosis [*N* (%)]	3 (15.8)	3 (60.0)	0 (0.0)	0 (0.0)	0 (0.0)	0 (0.0)

30 min. The peroxidase labeling was visualized with 0.2% 3,3′-diaminobenzidine (DAB) as chromogen. Sections were lightly counterstained with hematoxylin.

Semiquantitative assessment

TDP-43, tau, and Aβ pathologies in the amygdala, anterior and posterior portions of the entorhinal cortex, hippocampal dentate gyrus, CA1, 2, 3, and 4 regions, subiculum, fusiform gyrus, occipitotemporal gyrus were semiquantitatively evaluated using the following grading system blinded to any clinical or pathological information:

1. The total number of TDP-43-positive neuronal cytoplasmic inclusions (NCIs) in each anatomical region was assessed as follows: − no lesion, + one inclusion, ++ two or three inclusions, +++ four or five inclusions, ++++ 6–10 inclusions, +++++ 11 or over inclusions. In addition, the presence or absence of neuronal intranuclear inclusions (NIIs) and dystrophic neurites was also assessed. Then, we classified the topographic distribution of TDP-43 pathological changes using following system, which is similar to that reported by Amador-Ortiz et al. [2]: the amygdala type: inclusions were present only in the amygdala; the limbic type: inclusions extend to the amygdala, hippocampal dentate gyrus, CA1-4, entorhinal cortex, and fusiform gyrus, but not in the occipitotemporal gyrus; the temporal type: inclusions are present in the limbic system and also the in the occipitotemporal gyrus.
2. Tau-positive neuronal inclusions were counted in low power microscopic fields: 0, no tau-positive lesions; 1, one neuronal inclusion per few microscopic fields; 2, one inclusion in every field; 3, 4–30 inclusions in every field; 4, over 30 inclusions associated with numerous neurites in every field.
3. Aβ deposits were counted in low power microscopic fields: 0, no Aβ deposits; 1, two to three Aβ plaques in each field; 2, 4–10 Aβ plaques in each field; 3, 11–20 Aβ plaques in each field; 4, more than 20 Aβ deposits in each field.

Hippocampal sclerosis (HS) was defined by neuronal loss with gliosis in the hippocampal CA1 and/or subiculum, with relatively preserved neurons in the CA4, 3, and two regions and absence of intracellular and extracellular NFTs, or ischaemic changes that might explain neuronal loss in the CA1 and subiculum. HS was assessed blind to any clinical or pathological information.

Statistical analysis

The Mann–Whitney *U* test and Fisher's exact test were used to compare the demographic and pathological data between TDP-43-positive and TDP-43-negative groups in PSP and CBD series, respectively. Correlations between ratings of TDP-43 pathology and demographic data, or ratings of tau and Aβ pathologies in each anatomical region were assessed with Spearman's rank-order correlation statistic. Statistical analysis was performed using StatView for Macintosh program, version J-4.5. A value of $p < 0.05$ was accepted as significant.

Confocal laser scanning microscopy

Double-labeling immunofluorescence was performed with the combination of phosphorylation-dependent anti-TDP-43 (pAb pS409/410, rabbit, polyclonal, 1:1,000 [17]) and anti-tau antibodies (AT8, mouse, monoclonal, 1:500, Innogenetics, Ghent, Belgium). Sections from the amygdala and hippocampus in some PSP cases with TDP-43 pathology were pretreated by heating in a microwave oven for 5 min in 10 mM sodium citrate buffer, pH 6.0, at

100°C, allowed to cool then permeabilized with 0.2% (v/v) Triton X-100 in PBS. Following washing in PBS, non-specific antibody binding was blocked with normal sera and sections were incubated with a mixture of the two primary antibodies for 1 h at room temperature. After washing in PBS, sections were incubated with fluorescence-labeled secondary antibodies [AlexaFluor 488 anti-rabbit IgG (1:200) and AlexaFluor 555 anti-mouse IgG (1:200), Molecular Probes, Invitrogen, Paisley. UK]. After washing with PBS, sections were incubated with Toto-3 Iodide (Molecular Probes, Invitrogen, Paisley, UK) with 1 mg/ml RNase (Roche Diagnostics GmbH, Manheim, Germany) at 37°C. To quench (lipofuscin) autofluorescence, sections were incubated in 0.1% Sudan Black B for 10 min at room temperature and washed with 0.1% Tx-PBS for 30 min. Sections were coverslipped with Vectashield mounting media (Vector Laboratories Inc., Burlingame, CA, USA). Images were collected on a Leica TCS SP5 AOBS upright confocal (Leica Microsystems, Milton Keynes, UK) using the 488 nm (19%), 543 nm (30%) and 633 nm (60%) laser lines, respectively. To eliminate cross-talk between channels, the images were collected sequentially.

Immunoblotting

Frozen tissue from the amygdala, hippocampus, and frontal, temporal, and occipital cortices in one PSP case with TDP-43 pathology, one FTLD-TDP case (as a positive control) and eight negative controls (six PSP, one LBD, and one pathologically normal case) were prepared for western blotting according to methods previously described by Neumann et al. [31]. Briefly, 1 g of fresh frozen brain was homogenized in 5 ml/g (w/v) of low salt (LS) buffer-containing 10 mM Tris pH 7.5, 5 mM EDTA pH 8.0, 1 mM DTT, 10% (w/v) sucrose and Roche complete EDTA-free protease inhibitor. Homogenates were sequentially extracted with increasing strength buffers [Triton X-100 buffer (LS buffer + 1% Triton X-100 + 0.5 M NaCl), Triton X-100 buffer with 30% sucrose to float myelin, Sarkosyl buffer (LS buffer + 1% *N*-lauroyl-sarcosine + 0.5 M NaCl)]. Detergent-insoluble pellets were extracted in 0.25 ml/g Urea buffer (7 M Urea, 2 M Thiourea, 4% 3-[(3-Cholamidopropyl) dimethylammonio]-1-propanesulfonate (CHAPS), 30 mM Tris–HCl pH 8.5, Roche complete EDTA free protease inhibitor. Prior to SDS-PAGE immunoblot analysis, urea fractions were added in 1:1 ratio to SDS sample buffer (10 mM Tris pH 6.8, 1 mM EDTA, pH 8.0, 40 mM DTT, 1% SDS, 10% Sucrose, 0.01% Bromophenol Blue). Protein was resolved on 12% Tris–Glycine SDS-PAGE gels along with size standard (Bio-Rad kaleidoscope broad-range marker; Bio-Rad, Hercules, CA, USA). Proteins were transferred onto nitrocellulose membrane (Hybond ECL, GE Life Sciences, UK) and blocked for 1 h at 4°C in 5% (w/v) milk solution [5% powdered milk in Tris-buffered saline containing 0.1% Tween-20 (TBS-T)]. Membranes were incubated in phosphorylation-dependent mouse monoclonal antibody (mAb pS409/410, mouse, 1:1,000 [20]) for 1 h at room temperature followed by HRP-conjugated goat anti-mouse secondary antibody (Santa Cruz Biotechnology Inc, CA, USA). Antibodies were visualized by incubating in enhanced chemiluminescent reagent (ECL, GE Life Sciences) and imaged using the ImageQuant 350 system fitted with a F0,95 25 mm Fixed Lens (GE Healthcare, Life Sciences, UK). TDP-43 probed membranes were exposed for 5 min at different timeframes to obtain multiple images of differing intensity. Images were processed using ImageQuant TL software (GE Healthcare, Life Sciences, UK).

Results

Frequency and distribution of TDP-43 pathology

Clinical and pathological features for all subjects are shown in Table 1. TDP-43 pathology was noted in 5 of 19 PSP cases (26%) and in 2 of 12 CBD cases (17%). Disease duration, gender ratio and brain weight were not statistically different between PSP cases with and without TDP-43 pathology, or between CBD cases with and without TDP-43 pathology, respectively. Age at onset of disease (75 vs. 66 years) and age at death (82 vs. 74 years) tended to be higher, and dementia occurred more often, in PSP cases with TDP-43 pathology than in PSP cases without it (80 vs. 50%), although these differences did not reach statistical significance. One PSP case without TDP-43 pathology also had Lewy body pathology corresponding to brainstem-predominant type [26]. Ten PSP cases (3 TDP-43-positive and 7 TDP-43-negative cases) and four CBD cases (all were TDP-43-negative) had Aβ-positive diffuse plaques in the amygdala, hippocampus, and/or temporal cortex. Of the three TDP-43-positive PSP cases, one case had only a few neuritic plaques in the occipitotemporal gyrus. None of the PSP or CBD cases in our series fit the pathological criteria of AD [9, 28, 39].

In PSP cases, TDP-43-positive NCIs were most frequently noted in the amygdala and dentate gyrus granule cells in the hippocampus (5 cases, 100% of TDP-43-positive PSP cases), followed by the anterior portion of the entorhinal cortex (4 cases, 80%), subiculum (3 cases, 60%), posterior portion of the entorhinal cortex (3 cases, 60%), occipitotemporal gyrus (2 cases, 50%), fusiform gyrus (2 cases, 40%), and CA1 region (2 cases, 20%) (Table 2, Fig. 1a–d). In addition to the rounded inclusions noted in FTLD-TDP, all PSP cases had many irregular shaped

Table 2 Distribution of TDP-43 pathology in PSP and CBD cases

TDP-43 pathology												Hippocampal sclerosis (CA1/Subiculum)	Argyrophilic grains[b]
No.	Amygdala	ant.EC	DG	CA3/4	CA2	CA1	SB	post.EC	FG	OTG	TDP-43 distribution[a]		
PSP cases													
PSP1	++++	−	+	−	−	−	−	−	−	−	Limbic	−	−
PSP2	+++++	+++++	+++++	−	−	−	+	−	−	n	Limbic	+	−
PSP3	+++++	+++++	+++	−	−	−	++	++++	−	−	Limbic	−	−
PSP4	+++++	+++++	++	−	−	+	+++	+++++	+++++	+	Temporal	+	−
PSP5	+++++	+++	+++++	−	−	++	−	++	+++	+++	Temporal	+	Stage III
%	100.0	80.0	100.0	0.0	0.0	20.0	60.0	60.0	40.0	50.0		60.0	20.0
CBD cases													
CBD1	+++	++	−	−	−	−	−	n.a.	n.a.	n.a.	Limbic	−	−
CBD2	+++++	++	++++	++	−	+++++	+++++	++	−	−	Limbic	−	Stage II
%	100.0	100.0	50.0	50.0	0.0	50.0	50.0	50.0	0.0	0.0		0.0	50.0

The stages of TDP-43 pathology: −, no lesion in the anatomical region; +, 1 inclusion in the anatomical region; ++, 2–3 inclusions in the anatomical region; +++, 4–5 inclusion in the anatomical region; ++++, 6–10 inclusions in the anatomical region; +++++, 11 or over inclusions in the anatomical region. The stage of hippocampal sclerosis: −, no; +, mild; ++, moderate; +++, severe. The stage of argyrophilic grains: −, absent; +, present. ant.EC, the anterior portion of the entorhinal cortex; DG, hippocampal dentate gyrus; SB, subiculum; post.EC, the posterior portion of the entorhinal cortex; FG, fusiform gyrus; OTG, occipitotemporal gyrus

[a] The amygdala type: inclusions were present only in the amygdala; the limbic type: inclusions extend to the limbic system, but not in the occipitotemporal gyrus; the temporal type: inclusions are present in the limbic system and occipitotemporal gyrus as well

[b] The distribution of argyrophilic grains are assessed using a staging system proposed by Saito et al. [35]

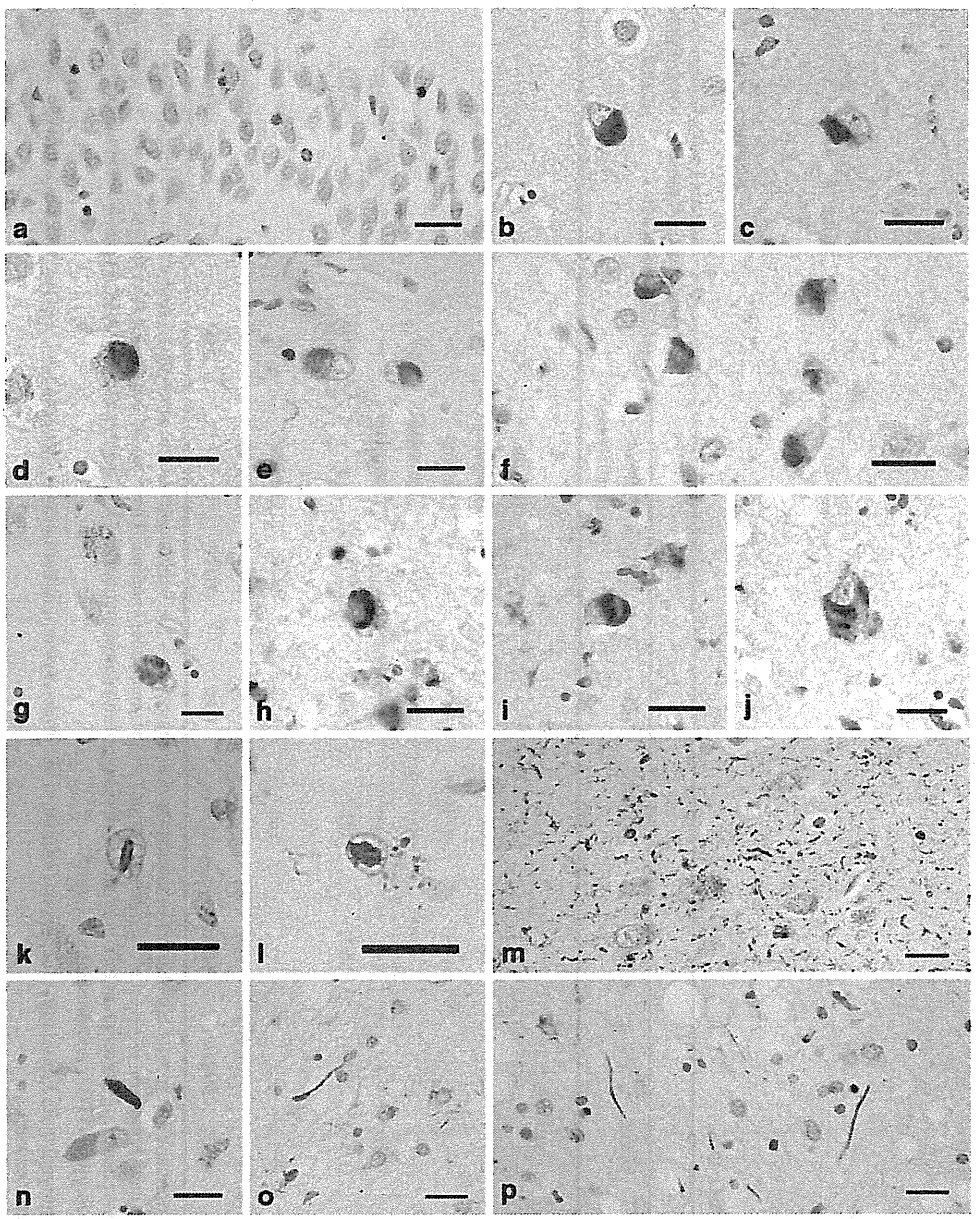

Fig. 1 TDP-43-positive lesions in PSP. **a** Neuronal cytoplasmic inclusions (NCIs) in the hippocampal dentate gyrus. **b–d** NCIs in the entorhinal cortex. Irregular shaped NCIs in the entorhinal cortex (**e**), fusiform gyrus (**f**), and subiculum (**g**). These inclusions have weakly stained or unstained regions. Small dot-like structures are also seen in the neuronal cytoplasm (**g**). Horseshoe-shaped (**h**, **i**) and NFT-like (**j**) NCIs in the entorhinal cortex. Intranuclear inclusions in the amygdala (**k**) and in the subiculum (**l**), cases PSP3 and PSP2, respectively. **m** Massive short threads-like structures in the subiculum, case PSP3. **n** Thick, thread-like structures in the amygdala. **o**, **p** Long, thin thread-like structures in the amygdala. pAb pS409/410 immunohistochemistry. All *scale bars* 20 μm

NCIs, such as flame-shape NFT-like, globose-type NFT-like, and horseshoe-like inclusions (Fig. 1e–j). One PSP case (PSP 2 in Table 2) showed a few NII in the subiculum (Fig. 1k, l). Two cases (PSP4 and PSP5) had abundant fine, short, thread-like structures immunopositive for TDP-43 from the CA1 to subiculum (Fig. 1m). TDP-43-positive thread-like structures were also observed in the amygdala (3 cases), entorhinal cortex (2 cases), CA1 (one case), and subiculum (one case) (Fig. 1n–p).

In two CBD cases, TDP-43-positive NCIs were observed in the amygdala, entorhinal cortex, hippocampal dentate gyrus, CA1, CA3/4, and subiculum (Table 2, Fig. 2a). The distribution of TDP-43 pathology was roughly consistent with that observed in PSP cases. NIIs were found in the subiculum and amygdala in one CBD case with severe TDP-43 pathology (Fig. 2b, c). Short thread-like structures immunopositive for TDP-43 were found in the amygdala, entorhinal cortex, CA1, CA3, and/or subiculum in both CBD cases with TDP-43 pathology. One CBD case had TDP-43-positive coiled body-like structures and thread-like structures in the alveus in the subiculum (Fig. 2d–f). Abnormal accumulation of TDP-43 was not found in the white matter of the temporal lobe and substantia nigra in any of the TDP-43-positive PSP or CBD cases.

Relationship between TDP-43 pathology and tau or Aβ burden

The ratings for tau burden in the TDP-43-positive PSP cases tended to be higher (but not significantly so) than

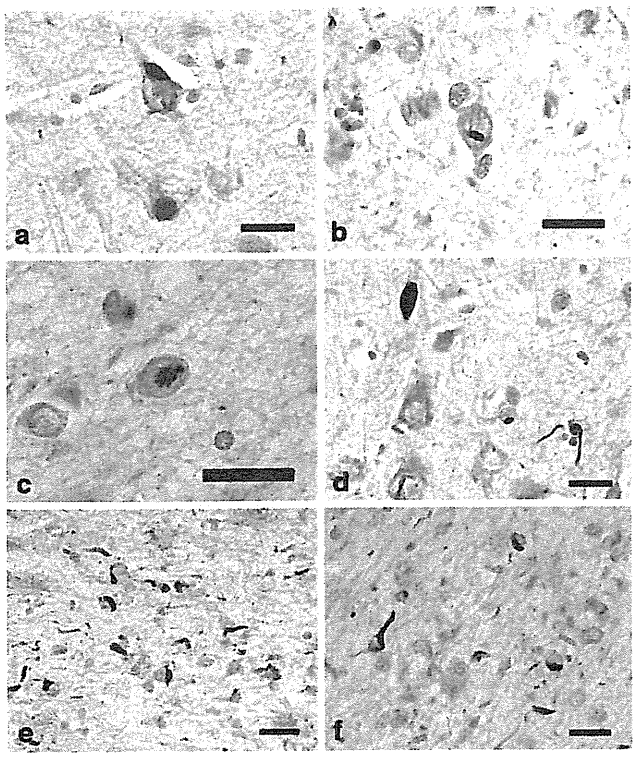

Fig. 2 TDP-43-positive lesions in CBD. **a** Neuronal cytoplasmic inclusions (NCIs) in CA3 region of hippocampus. **b**, **c** Neuronal intranuclear inclusions in the amygdala. **d** A thick neurite and thin, thread-like structures in the amygdala. **e** Short thread-like structures and glial cytoplasmic inclusions (GCIs) in the alveus in the entorhinal cortex. **f** Coiled body-like structures and GCis in the alveus in the entorhinal cortex. pAb pS409/410 immunohistochemistry. All *scale bars* 20 μm

those in the TDP-43-negative PSP cases, in almost all regions examined (i.e., including amygdala, entorhinal cortex, hippocampal dentate gyrus, CA1-4, fusiform gyrus, and occipitotemporal gyrus) (Fig. 3). In the PSP cases overall, rating for tau pathology in the occipitotemporal gyrus was significantly correlated with that of TDP-43 pathology ($r = 0.504$, $p < 0.05$), but no significant correlations between tau and TDP-43 ratings were found in any other regions. There were no significant differences in the degree of Aβ burden in any region between TDP-43-positive and TDP-43-negative PSP cases, and ratings for TDP-43 pathology did not correlate with those for Aβ burden in any region. Of three TDP-43-positive PSP cases having Aβ deposits, only one case had a few neuritic plaques in the occipitotemporal gyrus; however, this case did not have any TDP-43-positive inclusions in the region.

In the CBD cases, there were no significant differences in tau or Aβ burden in any region between TDP-43-positive and TDP-43-negative cases, and ratings for TDP-43 pathology did not correlate with those for tau or Aβ burden in any region.

Relationship of HS, argyrophilic grains, TDP-43 accumulation, and dementia

In 3 of 19 PSP cases (16%), evident neuronal loss in the CA1 and subiculum consistent with HS was noted (Fig. 4a, b). No CBD case showed HS. All three PSP cases with HS had a various degrees of TDP-43 pathology in the CA1 and/or subiculum (Fig. 4e–h), and two had extensive TDP-43

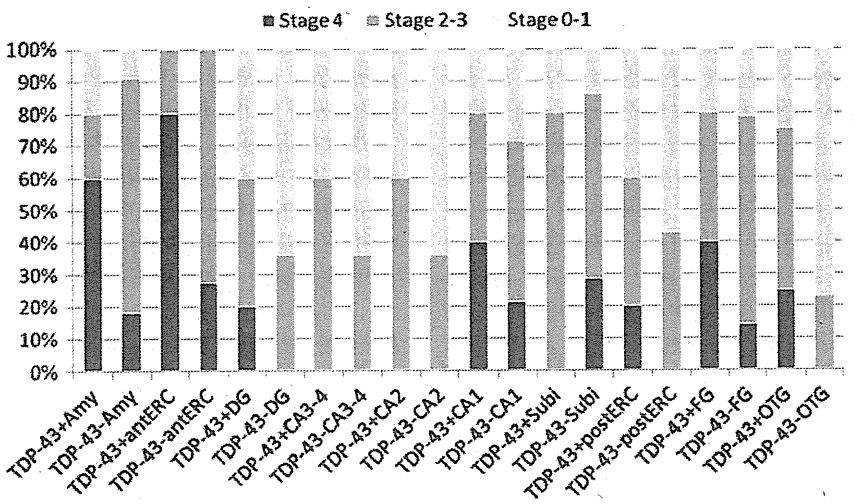

Fig. 3 Tau burden in the limbic system in PSP cases with and without TDP-43 pathology. In all regions but the subiculum, tau burden in PSP cases with TDP-43 pathology is more severe than that in PSP cases without TDP-43 pathology. Stage 0–1, no to mild tau deposition; stages 2–3, moderate to severe tau deposition; stage 4, very severe tau deposition (see detailed definition in the text). *TDP-43+* TDP-43-positive, *TDP-43−* TDP-43-negative, *Amy* amygdala, *antERC* the anterior portion of the entorhinal cortex, *DG* hippocampal dentate gyrus, *Subi* subiculum, *postERC* the posterior portion of the entorhinal cortex, *FG* fusiform gyrus, *OTG* occipitotemporal gyrus

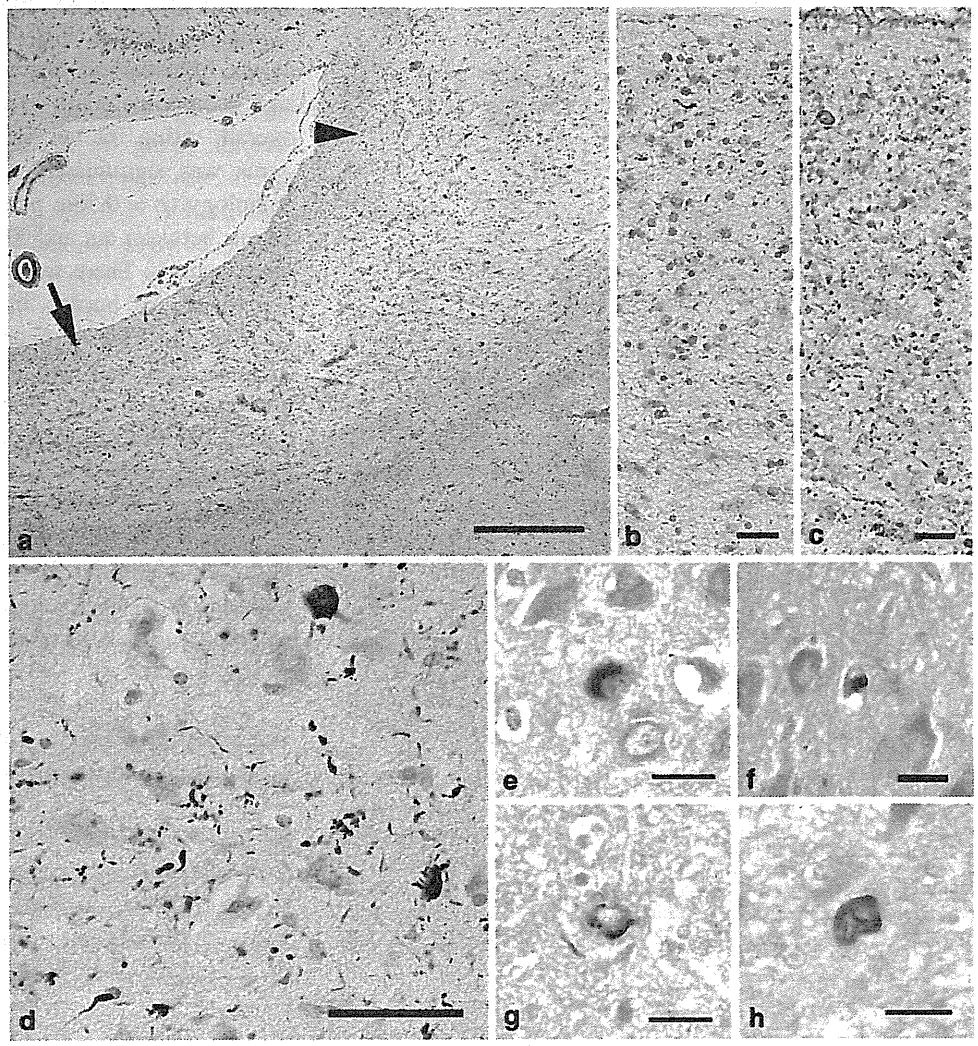

Fig. 4 Pathological features in the hippocampus in a PSP case with TDP-43, HS, and argyrophilic grains (PSP5). **a** A low power view of the hippocampal CA1 to subiculum. Severe reduction of the width with tissue rarefaction is noted in the subiculum (*arrow*) and to a lesser degree in the adjacent CA1 region (*arrowhead*). **b** A moderate power view of the subiculum on the same section as that shown in **a**. Severe neuronal loss associated with gliosis is evident. Argyrophilic threads and grains are scattered, but tangles are rare. **c** The subiculum on an adjacent section of **b**. A moderate number of tau-positive threads and grains, but only a few tangles, are seen. **d** Argyrophilic grains in CA1 region. **e**, **f** TDP-43-positive cytoplasmic inclusions in CA1 region. **g** An irregular shaped TDP-43 accumulation in the subiculum. **h** A coiled body-like TDP-43-positive inclusion in the subiculum. **a**, **b**, **d** Gallyas-Braak hematoxylin-eosin stain. **c** AT-8 immunohistochemistry. **e**–**h** pAb pS409/410 immunohistochemistry. *Scale bars* **a** 400 μm, **b**, **c** 25 μm, **d** 50 μm, **e**–**h** 20 μm

pathology in the limbic system: one case had both TDP-43 pathology and argyrophilic grains (Table 2). Two of the three PSP cases with HS had a few AT8-positive pretangles and argyrophilic grains in the CA1 and subiculum (Fig. 4b–d). Neurofibrillary tangles were rare in these regions in all PSP cases with HS (Fig. 4b). No significant ischemic changes in the hippocampal pyramidal neurons, or neuronal loss in the end plate, suggestive of a past history of severe epilepsy was noted in any of the PSP cases with HS. The frequency of HS in the TDP-43-positive PSP cases was significantly higher than that in TDP-43-negative PSP cases (60 vs. 0%, $p = 0.021$). Dementia was present in all of the 3 TDP-43-positive PSP cases with HS (100%), 4 of the 5 TDP-43-positive PSP cases with and without HS (80%), 1 of 2 TDP-43-positive PSP cases without HS (50%), and 7 of 14 PSP cases lacking both (50%). The frequency of dementia was not significantly different between PSP cases with and without HS ($p = 0.170$).

Concomitant argyrophilic grains were observed in four PSP (21%) and three CBD cases (25%) (Fig. 4d). Among these cases, one PSP and one CBD case had TDP-43 pathology (Table 2, Fig. 4e–h). There was no significant difference in the frequency of argyrophilic grains between TDP-43-positive and TDP-43-negative PSP cases, or between CBD cases with and without TDP-43 pathology, respectively. However, in the TDP-43-positive PSP and CBD cases, argyrophilic grains were found in those cases with the most severe TDP-43 pathology (Table 2).

Double immunofluorescence labeling in PSP cases

In the PSP cases examined, TDP-43 and tau pathologies were independently present in the perikarya of granular cells in the hippocampal dentate gyrus with no coexistence of these proteins (Fig. 5a–f). In contrast, in the amygdala, TDP-43 accumulation was often intermingled with tau accumulation in NCIs and dystrophic neurites, and colocalization was frequent (Fig. 5g–o). In the entorhinal cortex and parahippocampal gyrus in one PSP case with argyrophilic grains, many tau-positive grain-like structures

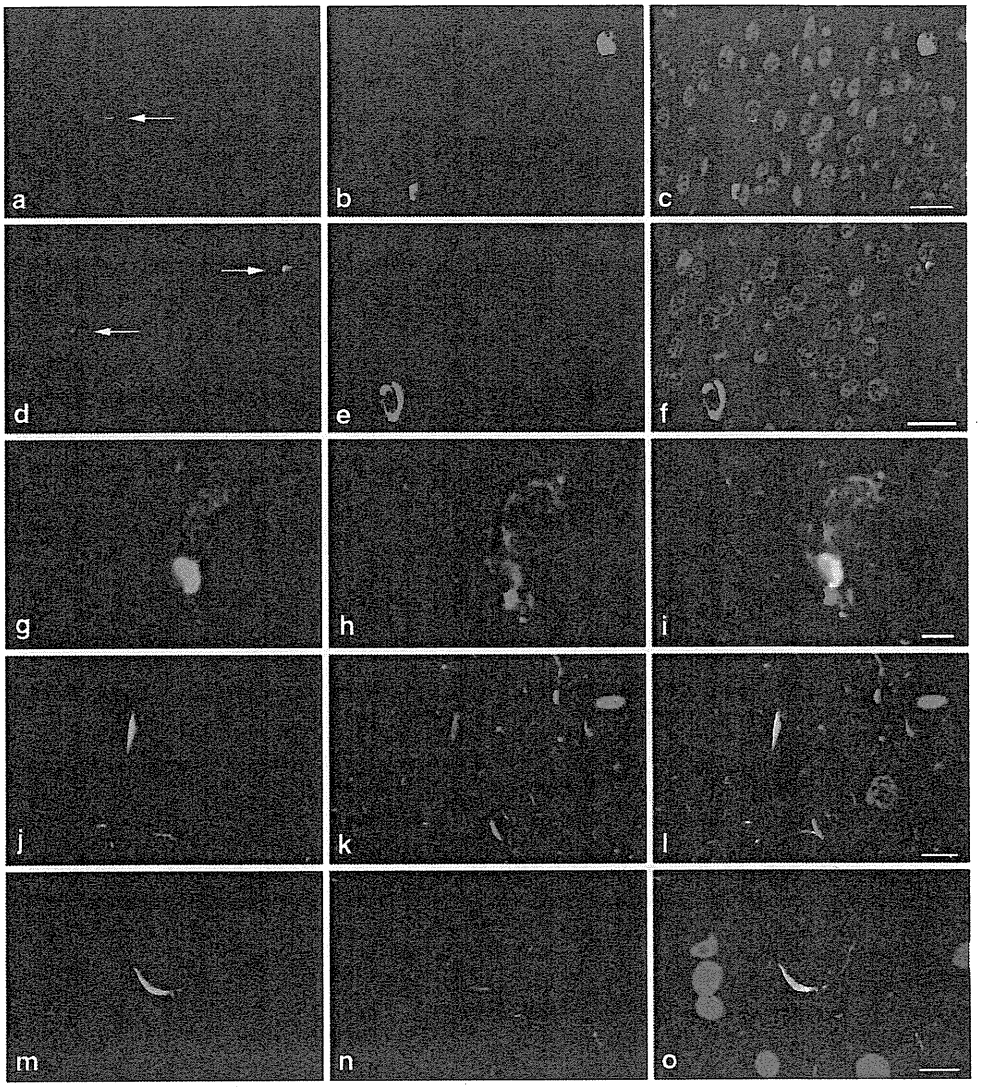

Fig. 5 Confocal double-imunofluorescence of TDP-43 (**a**, **d**, **g**, **j**, **m**) and tau (**b**, **e**, **h**, **k**, **n**) in PSP cases. *Merged images* are shown in **c**, **f**, **i**, **l**, and **o**. Blue fluorescence in merged images are nuclei. **a–f** In the hippocampal dentate gyrus, TDP-43 accumulation (*arrows*) is not colocalized with tau labeling. **g–i** In the amygdala, TDP-43 accumulation is often intermingled and colocalized with neuronal tau accumulation. **j–o** TDP-43-positive neurites (**j**, **m**) and many tau-positive neurites and granules (**k**, **n**) are seen in the amygdala. Coexistence of TDP-43 and tau is noted in some neurites (**l**, **o**). AT8 and pAb pS409/410 double immunofluorescence. *Scale bars* **a–c** 25 μm, **d–f** 25 μm, **g–i** 2.5 μm, **j–l** 7.5 μm, **m–o** 7.5 μm

were demonstrated, and TDP-43 was colocalized with tau in some of these structures (data not shown).

Biochemical analyses of TDP-43 in PSP cases

Immunoblot analysis of the sarkosyl-insoluble, urea-soluble fraction with mAb pS409/410 demonstrated distinct bands at (approximately) 45 and 25 kDa, as well as high molecular weight smears in the amygdala of a PSP case having TDP-43 pathology (Fig. 6, lane 6) and in the frontal cortex of a FTLD-TDP case (lane 5). Weak 25 and 45 kDa bands were also observed in the hippocampus in a PSP case, which had very mild TDP-43 pathology at this site (lane 7). Pathological TDP-43 bands and smear were not demonstrated in any of the other cases lacking TDP-43 pathology, including those with PSP (lanes 1 and 2) or Lewy body disease (lane 4), or in normal control cases (lane 3).

Discussion

This is the first study demonstrating abnormal accumulations of phosphorylated TDP-43 in the limbic system in a significant proportion (26%) of patients with PSP. Immunoblot analysis also demonstrated biochemical alterations in TDP-43 in tissue samples from a PSP case with TDP-43 pathology, similar to those in FTLD-TDP and ALS. Regional tau burden in PSP cases with TDP-43 pathology was higher than that in PSP cases without it, and TDP-43 burden was significantly correlated with that of tau in the occipitotemporal cortex. The frequency of HS in PSP cases with TDP-43 pathology was significantly higher than that in PSP cases without it. Collectively, these findings suggest that (1) PSP is one of the tauopathies in which pathological TDP-43 accumulation can occur in the limbic system, and (2) TDP-43 pathology may be associated with the occurrence of HS in PSP cases.

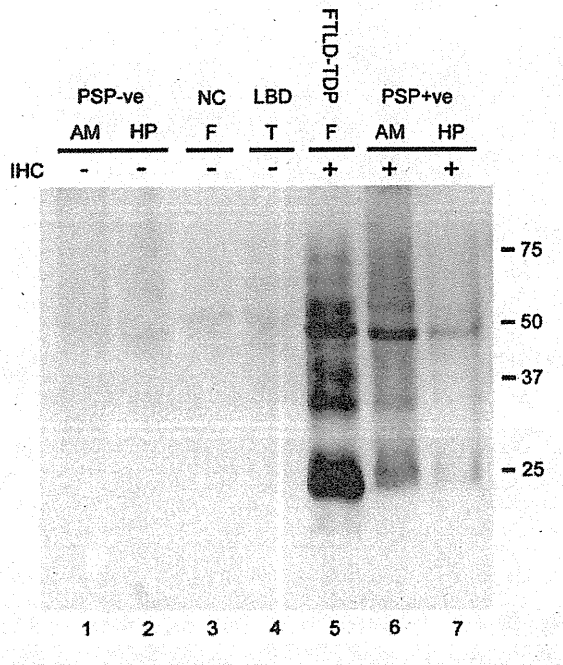

Fig. 6 Immunoblot analysis of the sarkosyl-insoluble fraction in representative PSP cases with phosphorylation-dependent monoclonal anti-TDP-43 antibody (mAb pS409/410). The 45 kDa full length TDP-43, 25 kDa fragments, and high molecular weight smear are strongly labeled in the amygdala of a PSP case with TDP-43 pathology (*lane 6*) and in the frontal cortex of a FTLD-TDP case (*lane 5*). Weakly stained 45 and 25 kDa bands are noted in the hippocampus of a PSP case (*lane 7*), in which TDP-43 pathology was mild. Similar 45 and 25 kDa bands and smears were not immunolabeled in any of the other cases without detectable TDP-43 pathology by immunohistochemistry (*lanes 1–4*). Normal 43 kDa TDP-43 is not stained by this phophorylation-dependent antibody in any case. *PSP* progressive supranuclear palsy, *LBD* Lewy body disease, *NC* normal control, *AM* amygdala, *HP* hippocampus, *F* frontal cortex, *T* temporal cortex, *IHC* pAb pS409/410 immunohistochemistry

Previous studies have demonstrated variable frequencies of concurrent TDP-43 pathology in many tauopathies: 23–56% in AD cases [2, 4, 40], 31–60% in DLB + AD cases [4, 30], 15% in CBD cases [40], and 60% in AGD cases [14]. Why no cases of PSP with TDP-43 pathology have previously been described is not clear. Our present findings show that, at least some, PSP cases may share a common pathophysiological background involving TDP-43 accumulation with other tauopathies with TDP-43 pathology. Several studies demonstrated that concurrent AD-type pathology was associated with the development of TDP-43 pathology in some neurodegenerative diseases [2, 4, 7, 14, 30]. However, it was unlikely that the development of TDP-43 pathology in our PSP series can be explained by the influence of Aβ deposits or neuritic plaques. For example, of all ten PSP cases having Aβ deposits, nine cases had only diffuse plaques, and the degree of Aβ deposition was not significantly different between TDP-43-positive and TDP-43-negative PSP cases and was not correlated with that of TDP-43 pathology in any regions. Although only one PSP case had a few neuritic plaques in the occipitotemporal gyrus, no TDP-43-positive inclusion was noted in the region.

Our findings are inconsistent with previous studies that failed to demonstrate immunohistochemical or biochemical abnormalities of TDP-43 in PSP cases [2, 3, 18, 40]. Considering that the sample size investigated in one of these previous studies [40] was far larger than that in our own study, the most plausible cause of the discrepancy may be the difference of the sensitivities of anti-TDP-43 antibodies employed: phosphorylation-dependent anti-TDP-43 antibodies do not stain normal nuclei, making true TDP-43-positive inclusions more readily identifiable [17, 37]. The distribution of TDP-43 pathology observed in our PSP cases was very similar to that reported previously in AD [2, 4, 18, 19, 40], DLB + AD [4, 30], and CBD [40], but tended to be more restricted than that in ALS/PDC of Guam [15, 16, 27]. Most frequently affected sites in these tauopathies are the amygdala and hippocampal dentate gyrus. Given these findings, it is plausible that the frequent TDP-43 accumulation in these sites in tauopathies is associated with some region-specific, rather than disease-specific, mechanism. On the other hand, it remains unclear whether TDP-43 is abnormally accumulated through an identical pathophysiological mechanism in various anatomical regions. For example, it was reported that abnormal TDP-43 accumulation was significantly correlated with the severity of tau pathology in AD cases [4] and Lewy body disease including many DLB + AD cases [30]. This same statistical relationship was observed in our PSP cases. Furthermore, in our present studies, TDP-43 was often colocalized with tau in NCIs and dystrophic neurites in the amygdala, although there were also TDP-43-positive but tau-negative lesions in this site. A coexistence of TDP-43 and tau in the same neuron in the amygdala and temporal cortex was also reported in AD and DLB cases in previous studies [4, 18]. However, in contrast to the amygdala, a coexistence of TDP-43 and tau in the same neuron in the hippocampal dentate gyrus was not seen in our PSP cases. This trend regarding non-colocalization of these two proteins was also noticed in the dentate granular cells in AD [40] and AGD brains [14]. This suggests that the mechanism underlying the accumulation of TDP-43 is different at least between the amygdala and hippocampal dentate gyrus, or that there is some unknown factor that can influence the occurrence of both TDP-43 and tau pathologies. In addition, considering the potential relationship between tau and TDP-43 in PSP presented in this paper, whether TDP-43 pathology is also noted in several other regions that are often involved by tau-associated lesions (e.g., the frontal cortex and basal ganglia) needs to be investigated in the future studies.

There is little known about the relationship between PSP and HS. In our series, 3 of 19 PSP cases (16%) had evident neuronal loss in the CA1 and/or subiculum consistent with the definition of HS. Furthermore, all of the cases with HS had TDP-43 pathology, and one of the three cases also had argyrophilic grains. It has been reported that HS cases have variable underling pathologies, including the 'pure form' of HS [1, 21, 34], FTLD-TDP [23], FTLD with motor neuron disease [29], AD [2], CBD [36], DLB [13], and AGD [5, 13]. Present findings support the possibility that the development of HS, at least in some PSP cases, may occur in association with concurrent TDP-43 pathology. On the other hand, whether the development of HS in PSP cases is correlated with the severity of tau or TDP-43 pathology remains unclear. Considering the relatively small size of the samples examined in the present study, the relationship between HS and TDP-43 accumulation in PSP, as well as the frequencies of these pathological features, needs to be confirmed in a larger case series.

Although influence of concurrent TDP-43 pathology on clinical features in tauopathies is not fully understood, some previous studies in AD, have demonstrated a comorbidity such that a concomitant TDP-43 pathology was associated with a later age at onset and death [4, 24], and significantly poorer cognitive function [24]. On the other hand, a study investigating a relatively small series of AGD did not demonstrate any significant difference in the age at death or disease duration between cases with and without TDP-43 pathology [14]. It is known that patients with PSP frequently exhibit psychiatric and behavioral disturbances, and that cognitive decline in PSP is associated with the atrophy in the orbitofrontal cortex [11] and more severe tau burden in the neocortex and hippocampus [6, 8, 22]. More recently, it was also reported that clinical presentation, including the occurrence of dementia, is influenced by the distribution and severity of tau pathology [42, 43]. In our PSP series, although not statistically significantly, the frequency of dementia in PSP cases with both TDP-43 and HS (100%), and that in all PSP cases with TDP-43 pathology (80%), were higher than that in PSP cases lacking both (50%). The potential co-morbid effect of concurrent TDP-43 pathology and/or HS on cognitive impairment in patients with PSP needs to be explored by further clinicopathological studies.

Acknowledgments This study was supported in part by a research grant from the Uehara Memorial Foundation and Grant No. AG13854 from the National Institutes of Health. We thank Ms. M. Onbe (Department of Neuropsychiatry. Okayama University Graduate School of Medicine, Dentistry and Pharmaceutical Sciences) for their excellent technical assistance, and the Parkinson's Disease Society Brain Bank for making available tissue samples for this study. A part of this study was presented at the 111th annual meeting of the British Neuropathological Society in January 2010.

References

1. Ala TA, Beh GO, Frey WH 2nd (2000) Pure hippocampal sclerosis: a rare cause of dementia mimicking Alzheimer's disease. Neurology 54:843–848
2. Amador-Ortiz C, Lin WL, Ahmed Z et al (2007) TDP-43 immunoreactivity in hippocampal sclerosis and Alzheimer's disease. Ann Neurol 61:435–445
3. Arai T, Hasegawa M, Akiyama H et al (2006) TDP-43 is a component of ubiquitin-positive tau-negative inclusions in frontotemporal lobar degeneration and amyotrophic lateral sclerosis. Biochem Biophys Res Commun 351:602–611
4. Arai T, Mackenzie IR, Hasegawa M et al (2009) Phosphorylated TDP-43 in Alzheimer's disease and dementia with Lewy bodies. Acta Neuropathol 117:125–136
5. Beach TG, Sue L, Scott S et al (2003) Hippocampal sclerosis dementia with tauopathy. Brain Pathol 13:263–278
6. Bigio EH, Brown DF, White CL 3rd (1999) Progressive supranuclear palsy with dementia: cortical pathology. J Neuropathol Exp Neurol 58:359–364
7. Bigio EH, Mishra M, Hatanpaa KJ et al (2010) TDP-43 pathology in primary progressive aphasia and frontotemporal dementia with pathologic Alzheimer disease. Acta Neuropathol (in press). doi: 10.1007/s00401-010-0681-2
8. Braak H, Braak E (1990) Neurofibrillary changes confined to the entorhinal region and an abundance of cortical amyloid in cases of presenile and senile dementia. Acta Neuropathol 80:479–486
9. Braak H, Alafuzoff I, Arzberger T, Kretzschmar H, Del Tredici K (2006) Staging of Alzheimer disease-associated neurofibrillary pathology using paraffin sections and immunocytochemistry. Acta Neuropathol 112:389–404
10. Cairns NJ, Neumann M, Bigio EH et al (2007) TDP-43 in familial and sporadic frontotemporal lobar degeneration with ubiquitin inclusions. Am J Pathol 171:227–240
11. Cordato NJ, Duggins AJ, Halliday GM, Morris JG, Pantelis C (2005) Clinical deficits correlate with regional cerebral atrophy in progressive supranuclear palsy. Brain 128:1259–1266
12. Davidson Y, Kelley T, Mackenzie IR et al (2007) Ubiquitinated pathological lesions in frontotemporal lobar degeneration contain the TAR DNA-binding protein, TDP-43. Acta Neuropathol 113:521–533
13. Dickson DW, Davies P, Bevona C et al (1994) Hippocampal sclerosis: a common pathological feature of dementia in very old (> or = 80 years of age) humans. Acta Neuropathol 88:212–221
14. Fujishiro H, Uchikado H, Arai T et al (2009) Accumulation of phosphorylated TDP-43 in brains of patients with argyrophilic grain disease. Acta Neuropathol 117:151–158
15. Geser F, Winton MJ, Kwong LK et al (2008) Pathological TDP-43 in parkinsonism-dementia complex and amyotrophic lateral sclerosis of Guam. Acta Neuropathol 115:133–145
16. Hasegawa M, Arai T, Akiyama H et al (2007) TDP-43 is deposited in the Guam parkinsonism-dementia complex brains. Brain 130:1386–1394
17. Hasegawa M, Arai T, Nonaka T et al (2008) Phosphorylated TDP-43 in frontotemporal lobar degeneration and amyotrophic lateral sclerosis. Ann Neurol 64:60–70
18. Higashi S, Iseki E, Yamamoto R et al (2007) Concurrence of TDP-43, tau and alpha-synuclein pathology in brains of Alzheimer's disease and dementia with Lewy bodies. Brain Res 1184:284–294
19. Hu WT, Josephs KA, Knopman DS et al (2008) Temporal lobar predominance of TDP-43 neuronal cytoplasmic inclusions in Alzheimer disease. Acta Neuropathol 116:215–220

20. Inukai Y, Nonaka T, Arai T et al (2008) Abnormal phosphorylation of Ser409/410 of TDP-43 in FTLD-U and ALS. FEBS Lett 582:2899–2904
21. Jellinger KA (2000) Pure hippocampal sclerosis: a rare cause of dementia mimicking Alzheimer's disease. Neurology 55:739–740
22. Jellinger KA (2008) Different tau pathology pattern in two clinical phenotypes of progressive supranuclear palsy. Neurodegener Dis 5:339–346
23. Josephs KA, Dickson DW (2007) Hippocampal sclerosis in tau-negative frontotemporal lobar degeneration. Neurobiol Aging 28:1718–1722
24. Josephs KA, Whitwell JL, Knopman DS et al (2008) Abnormal TDP-43 immunoreactivity in AD modifies clinicopathologic and radiologic phenotype. Neurology 70:1850–1857
25. Kabashi E, Valdmanis PN, Dion P et al (2008) TARDBP mutations in individuals with sporadic and familial amyotrophic lateral sclerosis. Nat Genet 40:572–574
26. McKeith IG, Dickson DW, Lowe J et al (2005) Diagnosis and management of dementia with Lewy bodies: third report of the DLB Consortium. Neurology 65:1863–1872
27. Miklossy J, Steele JC, Yu S et al (2008) Enduring involvement of tau, β-amyloid, α-synuclein, ubiquitin and TDP-43 pathology in the amyotrophic lateral sclerosis/parkinsonism–dementia complex of Guam (ALS/PDC). Acta Neuropathol 116:625–637
28. Mirra SS, Heyman A, McKeel D et al (1991) The Consortium to Establish a Registry for Alzheimer's Disease (CERAD). Part II. Standardization of the neuropathologic assessment of Alzheimer's disease. Neurology 41:479–486
29. Nakano I (1993) Temporal lobe lesions in amyotrophic lateral sclerosis with or without dementia—a neuropathological study. Neuropathology 13:215–227
30. Nakashima-Yasuda H, Uryu K et al (2007) Co-morbidity of TDP-43 proteinopathy in Lewy body related diseases. Acta Neuropathol 114:221–229
31. Neumann M, Sampathu DM, Kwong LK et al (2006) Ubiquitinated TDP-43 in frontotemporal lobar degeneration and amyotrophic lateral sclerosis. Science 314:130–133
32. Neumann M, Mackenzie IR, Cairns NJ et al (2007) TDP-43 in the ubiquitin pathology of frontotemporal dementia with VCP gene mutations. J Neuropathol Exp Neurol 66:152–157
33. Obi K, Akiyama H, Kondo H et al (2008) Relationship of phosphorylated alpha-synuclein and tau accumulation to Abeta deposition in the cerebral cortex of dementia with Lewy bodies. Exp Neurol 210:409–420
34. Probst A, Taylor KI, Tolnay M (2007) Hippocampal sclerosis dementia: a reappraisal. Acta Neuropathol 114:335–345
35. Saito Y, Ruberu NN, Sawabe M et al (2004) Staging of argyrophilic grains: an age-associated tauopathy. J Neuropathol Exp Neurol 63:911–918
36. Schneider JA, Watts RL, Gearing M et al (1997) Corticobasal degeneration: neuropathologic and clinical heterogeneity. Neurology 48:959–969
37. Schwab C, Arai T, Hasegawa M, Yu S, McGeer PL (2008) Colocalization of transactivation-responsive DNA-binding protein 43 and huntingtin in inclusions of Huntington disease. J Neuropathol Exp Neurol 67:1159–1165
38. Sreedharan J, Blair IP, Tripathi VB et al (2008) TDP-43 mutations in familial and sporadic amyotrophic lateral sclerosis. Science 319:1668–1672
39. The National Institute on Aging, and Reagan Institute Working Group (1997) Consensus recommendations for the postmortem diagnosis of Alzheimer disease. The National Institute on Aging, and Reagan Institute Working Group on diagnostic criteria for the neuropathological assessment of Alzheimer disease. Neurobiol Aging 18:S1–S2
40. Uryu K, Nakashima-Yasuda H, Forman MS et al (2008) Concomitant TAR-DNA-binding protein 43 pathology is present in Alzheimer disease and corticobasal degeneration but not in other tauopathies. J Neuropathol Exp Neurol 67:555–564
41. Van Deerlin VM, Leverenz JB, Bekris LM et al (2008) TARDBP mutations in amyotrophic lateral sclerosis with TDP-43 neuropathology: a genetic and histopathological analysis. Lancet Neurol 7:409–416
42. Williams DR, Lees AJ (2009) Progressive supranuclear palsy: clinicopathological concepts and diagnostic challenges. Lancet Neurol 8:270–279
43. Williams DR, Holton JL, Strand C et al (2007) Pathological tau burden and distribution distinguishes progressive supranuclear palsy-parkinsonism from Richardson's syndrome. Brain 130:1566–1576
44. Yokoseki A, Shiga A, Tan CF et al (2008) TDP-43 mutation in familial amyotrophic lateral sclerosis. Ann Neurol 63:538–542

Acta Neuropathol (2009) 117:151–158
DOI 10.1007/s00401-008-0463-2

ORIGINAL PAPER

Accumulation of phosphorylated TDP-43 in brains of patients with argyrophilic grain disease

Hiroshige Fujishiro · Hirotake Uchikado · Tetsuaki Arai · Masato Hasegawa · Haruhiko Akiyama · Osamu Yokota · Kuniaki Tsuchiya · Takashi Togo · Eizo Iseki · Yoshio Hirayasu

Received: 24 October 2008 / Revised: 18 November 2008 / Accepted: 18 November 2008 / Published online: 28 November 2008

Abstract To determine whether TAR-DNA binding protein 43 (TDP-43) immunoreactivity was present in brains of argyrophilic grain disease (AGD), we immunohistochemically examined 15 cases of AGD (mean age at death: 84 years) using a panel of anti-TDP-43 antibodies, including both phosphorylation-independent and -dependent ones. Nine AGD cases (60%) showed TDP-43 immunoreactivities mainly in the limbic regions and lateral occipitotemporal cortex. TDP-43 positive structures included neuronal cytoplasmic inclusions, dystrophic neurites, glial cytoplasmic inclusions, grain-like dot-shaped structures, and neurofibrillary tangle (NFT)-like structures. The distribution of these TDP-43 positive structures was largely consistent with that of argyrophilic grains. Double-labeling confocal microscopy revealed, however, that many of phospho-TDP-43 positive structures were not colocalized with phospho-tau staining. Colocalization of phospho-TDP-43 and phospho-tau was observed only in part of neuronal cytoplasmic inclusions, grain-like structures and NFT-like structures. There were no differences in demographics, disease duration, brain weight, NFT Braak stage, or severity of amyloid burden between AGD cases with and without TDP-43-immunoreactivity. However, cases of AGD with TDP-43-immunoreactivity were assigned to higher AGD stages than those without TDP-43-immunoreactivity ($P < 0.05$). Furthermore, the TDP-43 pathology tended to be prominent in cases with severe grain pathology. The results of the present study indicate for the first time a high frequency of concomitant TDP-43 pathology in AGD, and suggest that abnormal accumulation of TDP-43 may be involved in the pathological process and disease progression of AGD.

Keywords TDP-43 · Phosphorylation · Neurofibrillary tangles · Argyrophilic grain · Tau

H. Fujishiro · H. Uchikado · T. Arai (✉) · H. Akiyama · O. Yokota
Department of Psychogeriatrics, Tokyo Institute of Psychiatry,
2-1-8 Kamikitazawa, Setagaya-ku, Tokyo 156-8585, Japan
e-mail: arai@prit.go.jp

H. Fujishiro · H. Uchikado · T. Togo · Y. Hirayasu
Department of Psychiatry, School of Medicine,
Yokohama City University, 3-9 Fukuura, Kanazawa-ku,
Yokohama, Kanagawa 236-0004, Japan

M. Hasegawa
Department of Molecular Neurobiology,
Tokyo Institute of Psychiatry, 2-1-8 Kamikitazawa,
Setagaya-ku, Tokyo 156-8585, Japan

K. Tsuchiya
Department of Laboratory Medicine and Pathology,
Tokyo Metropolitan Matsuzawa Hospital, 2-1-1 Kamikitazawa,
Setagaya-ku, Tokyo 156-0057, Japan

E. Iseki
Department of Psychiatry,
Juntendo Tokyo Koto Geriatric Medical Center,
Juntendo University School of Medicine,
3-3-20 Shinsuna, Koto-ku, Tokyo 136-0075, Japan

Introduction

Argyrophilic grain disease (AGD) was first described by Braak and Braak [3] in the brains of patients with adult-onset dementia. Subsequently, many studies have revealed that argyrophilic grains (AGs) are not rare pathological features among old demented patients [4]. Recently, Togo et al. have classified AGD as four-repeat tauopathy such as progressive supranuclear palsy (PSP) and corticobasal degeneration (CBD), based on morphological, biochemical, and genetic analyses [28, 29]. AGD is neuropathologically

characterized by the presence of small spindle- or comma-shaped silver stain positive structures, so-called argyrophilic grains, in the neuropil in the limbic area, which includes the hippocampus, the entorhinal and transentorhinal cortices and the cingulate cortex [3, 4, 7].

TAR-DNA-binding protein 43 (TDP-43) was first identified as a major component of the ubiquitin-positive inclusions in sporadic frontotemporal lobar degeneration with ubiquitinated inclusions (FTLD-U), familial FTLD-U with progranulin gene mutations, and sporadic amyotrophic lateral sclerosis (ALS) [2, 22]. Subsequent studies found that ubiquitin-positive inclusions in familial FTLD-U with valosin-containing protein gene [23], familial FTLD with motor neuron disease linked to chromosome 9p [6], and SOD-1-unrelated familial ALS were positive for TDP-43 [19, 27]. Recent findings of various missense mutations of TDP-43 gene in familial and sporadic ALS cases prove an essential role of TDP-43 abnormality in neurodegeneration [10, 18, 26, 31, 32]. These disorders are now referred to as TDP-43 proteinopathy [2, 22].

TDP-43 immunoreactivity, however, has also been detected in other neurodegenerative disorders, including Alzheimer's disease (AD), Lewy body disease (LBD), Pick's disease, Guamanian parkinsonism–dementia complex (G-PDC), Guamanian ALS (G-ALS), hippocampal sclerosis, and Huntington's disease [1, 2, 8, 9, 11, 13, 21, 25]. Uryu et al. [30] have recently reported that TDP-43 immunoreactive pathology was detected in 15% of corticobasal degeneration (CBD) cases, but not in other primary tauopathies including progressive supranuclear palsy (PSP). It is unknown, however, whether TDP-43 positive structures are present in AGD, which belongs to the primary tauopathies as well [28]. To address this issue, in the present study, we immunohistochemically investigated 15 cases of AGD using a panel of anti-TDP-43 antibodies. Here, we show a high frequency of TDP-43 positive structures, which are associated with the severity of tau-positive grain pathology in AGD.

Materials and methods

Materials

A total of 15 cases of AGD were employed in this study. The neuropathologic diagnosis was confirmed through standardized neuropathological examinations, which included staining with hematoxylin–eosin, Klüver–Barrera, methenamine–silver and modified Gallyas–Braak methods, in multiple cortical and subcortical areas. All cases were assigned to both a Braak stage of neurofibrillary tangles (NFTs) and an AGD stage based upon the distribution of NFTs and AGs seen by modified Gallyas–Braak staining (Fig. 1a) [5, 7, 24]. The degree of amyloid burden was evaluated based upon Consortium to Establish a Registry for Alzheimer Disease (CERAD) guidelines [20]. All cases were obtained from brain banks at the Department of Psychogeriatrics, Tokyo Institute of Psychiatry and at the Department of Psychiatry, Yokohama City University School of Medicine. All AGD cases (mean age 84.0 years; range 75–97 years; 7 females and 8 males) showed a NFT Braak stage below III, suggesting that they do not have concomitant AD.

Screening with TDP-43 immunohistochemistry

The presence and severity of TDP-43 immunoreactivity were assessed in the amygdala, entorhinal cortex, hippocampus, lateral occipitotemporal gyrus, and inferior temporal gyrus, using 10% formalin-fixed and paraffin-embedded 6 μm thick sections in all AGD cases. In four of 15 cases, 4% paraformaldehyde (PFA)-fixed and frozen sections in 30 μm thickness were also available. Sections were incubated with 0.5% H_2O_2 for 30 min to eliminate endogenous peroxidase activity in the tissue. After washing sections with 0.01 M phosphate-buffered saline (PBS, pH 7.4) containing 0.3% TritonX-100 (Tx-PBS) for 30 min, they were blocked with 10% normal serum, then incubated for 72 h at 4°C with a previously well characterized antibody specific for phosphorylated TDP-43 (pS409/410) in Tx-PBS containing 10% normal serum [12]. After three 10-min washes in Tx-PBS, sections were incubated in a biotinylated secondary antibody for 1 h, and then in avidin–biotinylated horseradish peroxidase complex (ABC Elite kit, Vector Laboratories, Burlingame, CA, US) for 1 h. The peroxidase labeling was visualized with 0.01% 3,3′-diaminobenzidine (DAB) as a chromogen. The sections were counterstained briefly with hematoxylin. When the presence of TDP-43 immunoreactivity was noted, additional regions including caudate nucleus, putamen, cingulate gyrus, insula, and frontal and parietal cortices were also immunohistochemically examined for TDP-43. Immunopositive structures to pS409/410 were confirmed with other several phosphorylation-dependent and -independent anti-TDP-43 antibodies (Table 1) [12, 16]. Tau-positive structures were examined by immunostaining with anti-phosphorylated tau (clone AT8; 1: 3000, Innogenetics, Ghent, Belgium) (Fig. 1b) and anti-four-repeat tau (RD4; 1: 100, Millipore, Billerica, MA) (Fig. 1c). Double labeling immunofluorescence for phosphorylated TDP-43 (pS409/410) and phosphorylated tau (clone AT8; 1: 3000, Innogenetics, Ghent, Belgium) was performed using fluorescein isothiocianate (FITC)- and tetramethylrhodamine isothiocyanate (TRITC)-conjugated secondary antibodies; sections were examined with a confocal laser microscope (LSM5 PASCAL; Carl Zeiss MicroImaging gmbh, Jena, Germany).

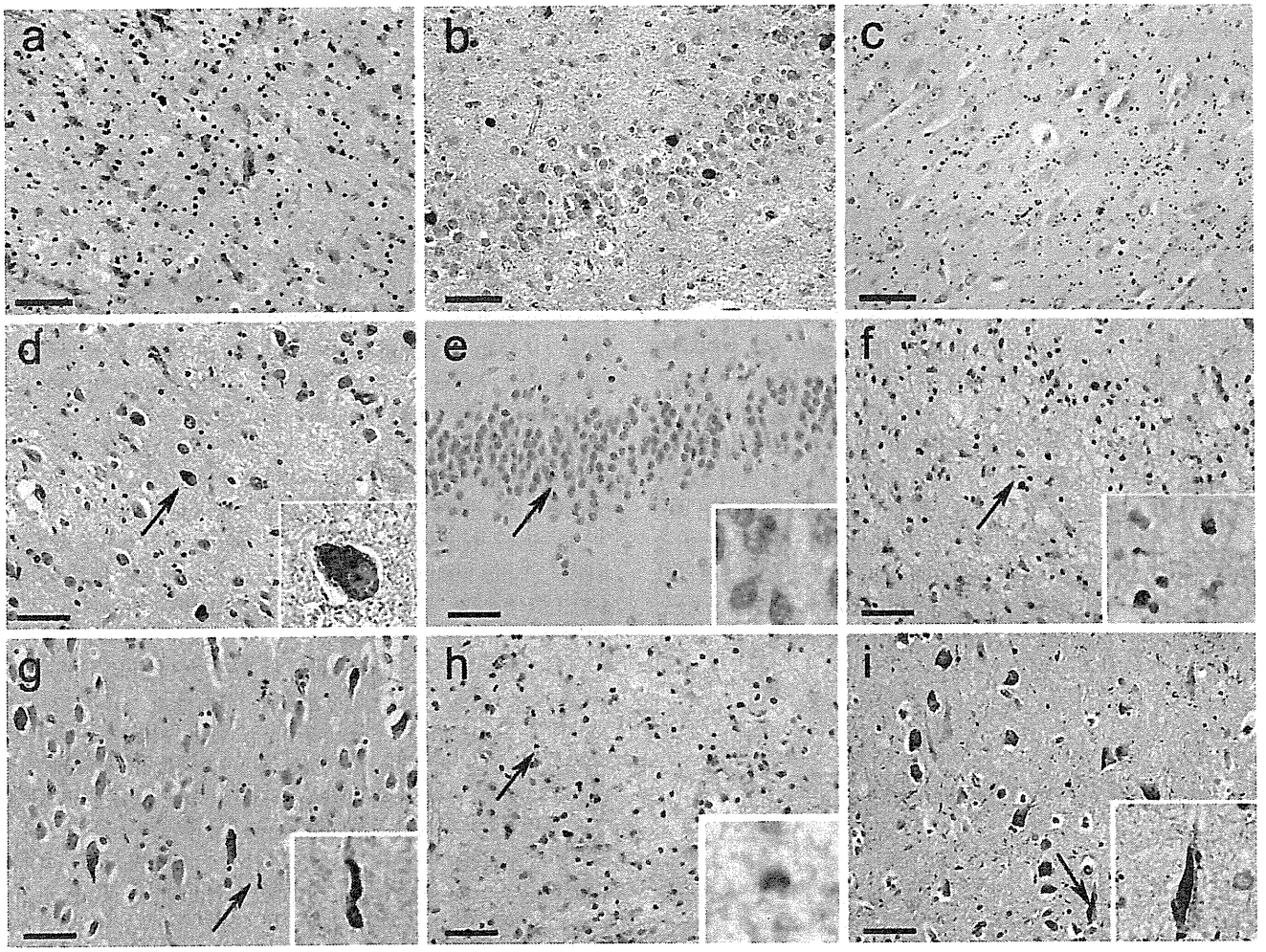

Fig. 1 Immunohistochemistry of argyrophilic grain disease using the phosphorylation-dependent anti-TDP-43 antibody (pS409/410). Modified Gallyas–Braak method (**a**) and immunostaining with anti-phosphorylated tau (**b**) and anti-four-repeat tau (**c**) show argyrophilic and tau-positive grains in amygdala (**a**) and CA1 region of hippocampus (**c**) and tau-positive neuronal cytoplasmic inclusions in the dentate granule cells (**b**). Phosphorylation-dependent TDP-43 immunohistochemistry reveals neuronal cytoplasmic inclusions (NCIs) (**d**, **e**), glial cytoplasmic inclusions (GCIs) (**f**) and dystrophic neurites (**g**). These are morphologically similar to TDP-43 positive structures observed in frontotemporal lobar degeneration with ubiquitinated inclusions (FTLD-U). Grain-like (**h**) and NFT-like (**i**) structures are also immunopositive. (**a**, **d**) amygdala, (**b**, **e**) dentate gyrus of hippocampus, (**c**, **i**) CA1 region of hippocampus, (**f**) lateral occipitotemporal cortex, (**g**) CA2 region of hippocampus, (**h**) entorhinal cortex. Each inset in a lower right corner represents a higher magnification of the region indicated by an *arrow* (*bars* 50 μm)

Table 1 Anti-TDP-43 antibodies used in this study

Antibody	Type	Antigen	Dilution
10782-2-AP (Protein Tech Group)	Rabbit	Recombinant protein (aa 1–260)	1:1,000
Anti-TDP43N [3–12]	Rabbit	EYIRVTEDENC (aa3–12)	1:1,000
pS409/410	Rabbit	CMDSKS(p)S(p)GWGM (aa 405–414)	1:1,000
pS403/404	Rabbit	NGGFGS(p)S(p)MDSKC (aa 398–408)	1:1,000
Anti-TDP43C (405–414)	Rabbit	CMDSKSSGWGM (aa 405–414)	1:1,000

Evaluation of severity and distribution of TDP-43 immunoreactivity in AGD

TDP-43 immunoreactive structures were examined on microscopic fields at 200× magnification in the amygdala, the entorhinal cortex, the striatum (putamen and caudate), the hippocampus (3 regions; CA1, CA2, and dentate gyrus), the cingulate gyrus, the insulated cortex, the lateral occipitotemporal cortex, and the inferior temporal cortex. TDP-43 immunoreactive structures were semi-quantitatively scored from (−) to (+++): (−) = absent; (+) = mild; (++) = moderate; (+++) = severe. TDP-43 immunoreactive

structures were separately evaluated as neuronal cytoplasmic inclusions (NCI), dystrophic neurites (DN) and glial cytoplasmic inclusions (GCI).

Statistical analyses

Data were analyzed with SigmaStat 3.5 (Systat Software, Inc., Point Richmond, CA, US), and the significance level was set at $P < 0.05$. To compare cases of AGD with and without TDP-43 immunoreactivity with respect to age at death, disease duration, brain weight, Braak NFT stage [5], CERAD plaque score [20], and AGD stage [7, 24], *t* test or Mann–Whitney Sum Rank Test was performed as appropriate. To compare cases of AGD with and without TDP-43 immunoreactivity, Fisher's exact test was performed with respect to sex ratio. According to CERAD criteria [20], amyloid burden was scored as follows; none: 0, sparse: 1, moderate: 2, frequent: 3. TDP-43 immunoreactivity was scored as follows; absence: 0, presence: 1. Relationships among pathological variables were assessed with Spearman's Rank Order Correlation.

Results

Distribution of TDP-43 immunoreactive structures and AGs

Prior to this study, we had produced several phosphorylation-specific anti-TDP-43 antibodies [12, 16]. These antibodies react only with abnormally deposited TDP-43 with no nuclear staining, making it easy for us to recognize abnormal findings. In this study, using these antibodies, we found various types of TDP-43 positive structures in nine of 15 AGD cases (60%). They include neuronal cytoplasmic inclusions, dystrophic neurites and glial cytoplasmic inclusions (Fig. 1d–g). In addition to these FTLD-U-like lesions, some grain-like structures were found to be positive for TDP-43 (Fig. 1h). Various amounts of TDP-43 immunoreactive NFT-like structures were also observed (Fig. 1i). There was no neuronal intranuclear inclusion in this series. These TDP-43 positive structures were mainly detected in the amygdala, entorhinal cortex, hippocampal CA1, subiculum and lateral occipitotemporal cortex. Of these regions, the amygdala and adjacent entorhinal cortex showed the most intense TDP-43 immunoreactivity. TDP-43 positive neuronal cytoplasmic inclusions in the dentate gyrus of the hippocampus, which is one of the features of FTLD-U, were observed in only two of nine cases with TDP-43 immunoreactivity.

The distribution and severity of TDP-43 immunoreactive structures were largely parallel with that of AGs, as detailed in Table 2. For instance, both TDP-43 positive structures and tau positive AGs were relatively confined to the amygdala and anterior parahippocampal gyrus in cases 1–5, and they extended to the temporal neocortices in cases eight and nine. Furthermore, cases 7–9 exhibited TDP-43 immunoreactive pathology in the pyramidal neurons in the CA2, where NFTs are common in AGD but not in AD [17]

Table 2 AGD staging and distribution of TDP-43-immunoreactive pathology

	AGD staging	AMY	Parahippocampal gyrus	Hippocampus			CIG	INS	OTC	ITC	CP
			(ant/post)	CA1	CA2	DG	(ant/post)	(ant/post)	(ant/post)	(ant/post)	
#1	I	NCI+, GCI+	NCI+, DN+, GCI+/0	NCI++	0	0	0/0	0/0	0/0	0/0	0
#2	I	NCI+, DN+	NCI+, GCI+/0	0	0	0	0/0	0/0	NCI++, GCI+/0	0/0	0
*#3	II	0	0	NCI+	0	0	0/0	0/0	0/0	0/0	0
#4	II	NCI+, GCI+	NCI+, GCI+/0	0	0	0	0/0	0/0	0/0	0/0	0
#5	II	NCI ++, GCI +	NCI++, GCI +/0	NCI++	0	0	0/0	0/0	NCI+, GCI+, DN+/0	0/0	0
#6	III	NCI+	NCI+, DN+, GCI+/DN+	NCI+	0	0	0/0	0/0	NCI+, GCI+, DN+/0	0/0	0
#7	III	NCI+++, GCI++	NCI+++, GCI++, DN+/NCI+++, GCI++, DN+	NCI++	NCI+	0	0/0	NCI+/0	NCI++, GCI++, DN+/NCI+	0/0	0
#8	III	NCI++, GCI +	NCI++, GCI+/NCI++	NCI++	NCI+, DN+	NCI+	NA	NCI+/0	NCI+/NCI+	NCI+/0	0
#9	IV	NCI++, DN++, GCI+	NCI+, DN++, GCI+/NCI+, DN+	NCI+	NCI+	NCI+	0/0	0/0	NCI+, DN++, GCI+/NCI+, DN++	DN+/0	0

AMY amygdala, *CIG* cingulated gyrus, *INS* insula, *OTC* occipitotemporal cortex, *ITC* inferior temporal cortex, *CP* caudate/putamen, *ant* anterior, *post* posterior, *NCI* neuronal cytoplasmic inclusions, *GCI* glial cytoplasmic inclusions, *DN* dystrophic neurites, *NA* not available, – absent, + mild, ++ moderate, +++ severe, *in this case (#3), there is a discrepancy of TDP-43 immunoreactivity between formalin-fixed paraffin-embedded sections and paraformaldehyde-fixed floating sections (see "Results"; Fig. 4)